X-692-71-400

TM X- 65739

THE SOLAR ENVELOPE

L. F. BURLAGA

OCTOBER 1971

GSFC

GODDARD SPACE FLIGHT CENTER

GREENBELT, MARYLAND

THE SOLAR ENVELOPE

by

L. F. Burlaga
Laboratory for Extraterrestrial Physics
NASA Goddard Space Flight Center
Greenbelt, Maryland

November 1971

THE SOLAR ENVELOPE

I. Introduction

II. Structure

- A. Radial Variations
- B. Azimuthal Variations
- C. Time Variations

III. Physical Processes in the Envelope

- A. Cosmic Ray Scattering
- B. Acceleration and Heating in the Envelope
  - 1. Acceleration by Heating
    - a. Some Basic Facts
    - b. General Theory
    - c. Wave Damping Theory
  - 2. Acceleration by Waves
  - 3. Acceleration by the Magnetic Field
- C. Angular Momentum Transfer

IV. Discussion

Abstract

Processes which occur within the region between $\approx 2R_\odot$ and $25R_\odot$, which is called the solar envelope, probably have an important effect on the solar wind as seen at 1 AU. In the envelope the wind speed becomes supersonic and super-Alfvenic, the magnetic energy density is larger than the flow energy density, and the magnetic energy density is much larger than the thermal energy density. Large azimuthal gradients in the bulk speed are expected in the envelope, but the stream interactions near the outer edge of the envelope are probably relatively small.

Cosmic ray observations suggest the presence of hydromagnetic waves in the envelope. The collisionless damping of such waves could heat protons out to $\approx 25R_\odot$ and thereby cause an increase in V and T_p consistent with the observed T_p-V relation. A mechanism which couples protons and electrons would also heat and accelerate the wind. Alfven waves can accelerate the wind in the envelope without necessarily causing heating of protons; the Lorentz force might have a similar effect.

Magnetic stresses cause an increase in V_φ which reaches a maximum in the envelope. Viscous stresses would also increase V_φ, but their importance is controversial.

Observations at 1 AU are not sufficient to determine the relative importance of the various processes that might occur in the envelope. Space probes which descend close to the envelope should significantly increase out understanding of such processes.

Page intentionally left blank

I. Introduction

Several types of evidence suggest that a variety of physical processes which are important in the formation of the solar wind occur in the region between $\approx 2R_\odot$ and $\approx 25R_\odot$. This region, called the solar envelope, bridges the gap between the interplanetary medium and the lower corona (Figure 1). Unlike the interplanetary medium, which has been studied directly by space probes to .7 AU, and unlike the lower corona, which has been extensively studied by various indirect methods, this intermediate region has remained largely inaccessible to observations. Yet it undoubtedly holds the answers to many of the unsolved problems in solar wind theory and solar-terrestrial relations, and it is probably the site of novel and interesting physical processes.

The observations near 1 AU and at the sun provide valuable clues to the nature of the processes occurring near the sun, but they are not sufficiently restrictive to unambiguously identify the most important processes governing acceleration, heating, energy transport, and angular momentum transport in the envelope. In fact, there are competing theories for each of these processes. Without a satisfactory physical understanding of the processes one cannot derive an accurate model for the fluid parameters in the envelope. However, one can obtain an estimate of these parameters using models designed to explain the "quiet time" solar wind at 1 AU and from this one can obtain estimates of the parameters that govern the general physical processes in the envelope. This and the question of azimuthal and temporal variations in the envelope are the subjects of Section II.

Section III contains a general discussion of the physical processes which might occur in the envelope. It begins with a discussion of cosmic ray propagation in the envelope, since the existence of an envelope was

suggested by cosmic ray observations. These observations indicated a region of hydromagnetic wave activity near the sun. The range of solar wind speeds and the observed relations between the wind parameters and V suggest physical processes in the envelope other than Coulomb interactions. Several physical processes which might accelerate and heat the wind are discussed in IIIB; all of these processes occur in the envelope. Finally, the effects of the magnetic field and viscosity on the azimuthal wind speed, which is expected to be a maximum in the envelope, are considered in IIIC.

II. Structure

A. Radial Variations

The conditions at 1 AU and thus presumably also in the envelope are constantly changing, so a solar wind model can refer to any one of an infinite number of states at 1 AU. We shall restrict the discussion to some models which are designed to explain a "quiet" solar wind state, defined by Hundhausen (1968). It is important to understand that this is just one of an infinite number of states. Because n and T_p are related to V, the quiet wind temperature and density are defined by specifying V alone, V=320 km/sec. This does not correspond to the average speed, most probable speed, etc; it is a state between the lowest speeds ($\approx$250 km/sec) and the probable speed ($\approx$400 km/sec).

The density n(r), and magnetic intensity B(r), are not very sensitive to the thermodynamic properties of the solar wind and can be estimated using a 1-fluid model. Figure 2 shows n(r) and B(r) obtained by Whang (1970a); they are both monotonically decreasing functions. Whang's "quiet-time" density is consistent with the indirect measurements between $2R_\odot$ and $20R_\odot$ and with the direct measurements ($8/cm^3$) at 1 AU. His magnetic field is somewhat higher at the sun and 1 AU than the typical measured values (2G at the sun compared to the value 1G which is usually quoted, and 7.3γ at 1 AU compared to the observed value, 5γ), but his B(r) is adequate for the accuracy that we are concerned about.

Temperatures present a greater problem, since thermodynamically the solar wind consists of 2-fluids and the transport parameters governing transfer of energy and momentum are not known for a magneto-plasma such as the solar wind. We shall use 2 competing models which make distinctly

different assumptions about the physical processes that determine the proton temperature T_p and the electron temperature T_e - the model of Hartle and Barnes (1970) and the model of Wolff et al. (1971).

The proton temperature profiles predicted by the two models are shown in Figure 3. They both predict the same T at 1 AU, but their description of the envelope is quite different. Hartle and Barnes predict a nearly isothermal region between $3R_\odot$ and $25R_\odot$, ($4\times10^5 \lesssim T \lesssim 8\times10^5{}^oK$) because they assume an extended non-thermal proton heat source with characteristic size $b=26R_\odot$. On the other hand, Wolff et al. predict a power law decrease between $3R_\odot$ and $\approx20R_\odot$, from $T = 1.2\times10^6{}^oK$ to $2\times10^5{}^oK$; they obtain the quiet time temperature at 1 AU by postulating an isothermal region with $T_e=T_p=1.2\times10^6{}^oK$ out to $3R_\odot$ and by introducing viscous heating which becomes important at $\gtrsim20R_\odot$. The temperature rise due to viscous heating is based on the use of the Braginskii (1965) formula for viscosity, $\eta=9\times10^{-17}T_p^{5/2}$ in cgs units. It has been argued (Parker, 1965; Hartle and Barnes, 1970) that this is not applicable in the region where viscous heating is said to be important and that the actual viscosity is negligible.

The electron temperature at $\approx2R_\odot$ is $\approx1.5\times10^6K$ and at 1 AU is $\approx1.5\times10^5K$. Models which use the Chapman thermal conductivity predict unacceptably high T_e and conduction flux at 1 AU ($\approx3\times10^5{}^oK$) (Hundhausen, 1969), but models which reduce the conductivity can predict a lower T_e at 1 AU (Wolff et al. 1971). Figure 4 shows $T_e(r)$ predicted by Wolff et al. (1971) on the assumption that $K_e=K_{ec}(r/R_\odot)^p$ where K_{ec} is the Chapman conductivity $K_{ec}=5.5\times10^9T_e^{5/2}$ and p is a free parameter which is taken to be $p=-.728$. A straight line is drawn between 1.5×10^6K at $2R_\odot$ and 1.5×10^5 at 1 AU in Figure 4 as an alternate $T_e(r)$ profile.

The relative importance of the two kinds of internal energy - the magnetic energy density $B^2/8\pi$ and the thermal energy density $nk(T_p+T_e)$ - is shown in Figure 5 which gives a plot of $\beta_T = nk(T+T_e)/(B^2/8\pi)$ as a function of r. This is based on the density profile in Figure 2, the empirical $T_e(r)$ in Figure 4, the $T_p(r)$ obtained by Hartle and Barnes (1970) and shown in Figure 3, and values of B(r) somewhat reduced from those in Figure 2. β_T increases from a very low value at $2R_\odot$ ($\beta\approx.1$) to $\gtrsim 1$ at $\approx 50R_\odot$. If the Wolff et al. (1971) model for $T_p(r)$ were used $\beta_T(r)$ would be somewhat higher at small r and lower at higher r. The proton $\beta(r)$, $\beta_p=nkT/(B^2/8\pi)$, shows the same general features as β_T, but is somewhat smaller (Figure 5).

The relation between the total internal energy density and the flow energy density is shown as a function of r in Figure 6. Below $\approx 15R_\odot$ the internal energy, which is mostly magnetic, is dominant. Above $\approx 15R_\odot$ the flow energy is dominant.

Figure 7 shows the 3 characteristic speeds of the solar wind - the Alfven speed, $V_A=B/\sqrt{4\pi\rho}$, the sound speed, $V_S=\sqrt{\gamma p/\rho}$, and the perpendicular magnetoacoustic speed, $V_M=(V_A^2+V_S^2)^{1/2}$ as a function of $r/R_\odot$, together with the bulk speed V(r) given by Hartle and Barnes (1970). The details of this figure depend on the particular models, but illustrates the following general results: 1) The flow becomes supersonic at $\approx 6R_\odot$; 2) V becomes comparable to V_A and V_M in the region between $10R_\odot$ and $20R_\odot$; 3) When $r\lesssim 5R_\odot$ $V_A\approx V_M>>V_S>>V$; 4) When $r\gtrsim 20R_\odot$, $V>>V_M>V_A\approx V_S$; 5) Near $15R_\odot$, $V\approx V_S\approx V_A$.

B. Azimuthal Variations

The models discussed above are steady state, symmetric models. Generally, neither of these assumptions is valid for the solar wind. The high speed streams which recurred at 27 day intervals in 1962 (Neugebauer and Snyder, 1966) clearly indicate azimuthal variations in the wind structure. Evidence for azimuthal gradients at 1 AU has also been found using widely separated spacecraft at ≈1 AU. Presumably, similar variations in the bulk speed also occur in the envelope.

Models which would make it possible to extrapolate from observations of the azimuthal structure at 1 AU to the envelope do not exist. However, there are some idealized models which give insight into the development of the azimuthal structure.

Carovillano and Siscoe (1969) considered a linear, polytropic model with sinusoidal velocity perturbations of V_r and no variations in n and V_φ at an inner boundary at $20R_\odot$. Since this model specifies the conditions near the edge of the envelope, it cannot be used to predict conditions there, but the general results are still significant. They predict sinusoidal perturbations in the density and azimuthal speed, growing linearly with distance from the sun. The model predicts that V_φ and V_r should be anticorrelated and that ρ should lead V_r by $\pi/(8\Omega)$, where Ω is the solar rotation rate and 4 streams are assumed. This qualitatively shows the observed snow-plow effect on density and the observed stream deflection, but the actual phase relations differ in magnitude from those predicted and the observed asymmetry in the $V_r(t)$ profile is not predicted. Nevertheless, the model indicates that the effects of stream interactions should be nearly linear near the edge of the envelope. In particular it will be easier to measure the V_φ due to co-rotation if one is near the

envelope, since the contribution to V_φ from the stream interaction will be small there. Density perturbations will also be smaller near the envelope, so it will be easier to study the effect of solar boundary conditions on density with data from a spacecraft close to the sun.

A generalization of the Carovillano-Siscoe model which includes non-linear effects was presented by Goldstein (1971). The results are illustrated in Figure 8. Near 1 AU, the model predicts the observed asymmetry on V_r, the strong density peak at the leading edge of the stream, and the observed form (Siscoe, 1971) of V_φ. Clearly, non-linear effects are important at 1 AU. This point was also made by Burlaga et al. (1971). Closer to the sun, however, the results closely resemble those of the linear model.

C. Time Variations

It has long been known that the solar wind is highly variable in time, since ≈27 day recurring patterns are usually not seen in the plasma parameters (e.g., see Figure 2 in Burlaga and Ogilvie, 1970a). Gosling and Bame (1971), analyzing Vela data from 1964 through 1967, found that few streams endure for more than 2 solar rotations and that the characteristic time for speed changes is about 3 days. Similar variations must occur in the envelope.

The effect of a symmetric time variation in the temperature at .1 AU (a linear increase from 6×10^5°K to 1.6×10^6°K in ≈50 hrs. followed by a corresponding decrease)was studied by Burlaga et al. (1971) using the spherically-symmetric 1-fluid model of Hundhausen and Gentry (1969). They found an asymmetric response at 1 AU due to non-linear interactions (Figure 9). The general features of this profile are consistent with

observations, suggesting that non-linear, adiabatic compression may be a basic characteristic of stream interactions. Similar non-linear effects are produced by a time varying spherically symmetric wind and by an inhomogeneous, stationary wind, so it is difficult to distinguish these two states; measurements of V_φ are very important in this regard.

The effect of a linear increase in the solar wind speed at ≈.1A over ≈50 hr was studied by Formisano and Chao (1971) using a spherically-symmetric model. They too found a non-linear interaction near 1 AU, and noted that the fast stream generates a pressure pulse which ultimately forms a shock pair at $\gtrsim$ 1 AU. This mechanism is not likely to produce shocks in the envelope.

Non-linear interactions have important effects on the meso structure of the solar wind, but they are probably perturbations on the macroscale properties (Burlaga and Ogilvie, 1970 a,b). For example, Figure 10 from Burlaga and Ogilvie, 1970a shows the distribution of positive and negative ΔV, the difference between consecutive 3-hour average values of bulk speed, for the interplanetary observations of Explorer 34; there is a difference between positive and negative gradients, presumably largely due to non-linear interactions, but the difference is relatively small. Similarly, the average wind speed, is probably not greatly changed by non-linear interactions, and the effect on the distributions of n and T is probably a skewing (Burlaga and Ogilvie, 1970 a,b) which does not greatly affect the long term averages. It will be interesting to compare the shapes of the distributions of n and T at .3 AU and at 1 AU.

III. Physical Processes

A. Cosmic Ray Diffusion in the Envelope.

Relativistic protons were emitted in an explosive solar flare on Feb. 23, 1956, and were observed at the earth by Meyer et al. (1956). Lust and Simpson (1957) noted three interesting effects in these observations: 1) The actual travel time of the particles was only a few minutes longer than the direct propagation time, 2) The particles arrived anisotropically from the sunward direction, 3) The more energetic particles arrived earlier than the less energetic particles, even though they were all propagating at essentially the same speed c. The first effect implies that particles were delayed in some region between the earth and the sun. If the delay were due to diffusion near the earth, then the particles would not have arrived anisotropically, so it is argued that they were delayed in a region near the sun. Now, there are 2 possibilities: Either the particles were trapped, for example by steady magnetic fields such as the magnetic field bottles identified by Schatten (1970) or by discontinuity surfaces (Fisk and Schatten, 1971), or they were delayed by diffusing in a fluctuating magnetic field. Lust and Simpson (1957) showed that the observed dispersion of onset times (effect 3) can be explained by diffusion in the region between the sun and $\lesssim 60 R_\odot$. They called the region the solar envelope.

Although the Feb. 23, 1956, event suggested the existence of an envelope filled with MHD waves, it did not provide a precise estimate of the size of the envelope, because all but the early minutes of the event were dominated by the effects of interplanetary scattering, as is the case for most events.

The May 4, 1960 event (McCracken, 1962) was ideal for studying the envelope because there was a strong anisotropy at 1 AU throughout the event, indicating that there was negligible scattering in the interplanetary medium at that time. Thus, the interplanetary "veil" was momentarily raised and we could "see" the envelope directly. Burlaga (1970) presented a theory for propagation under such circumstances which accurately describes the intensity-time profile (Figure 11). It gives $R_E \approx 25 R_\odot$ for the characteristic size of the envelopeand $D_E \approx 10^{21} cm^2/sec$ for the diffusion coefficient. Duggal et al. (1971) applied the same model to the event of Nov. 18, 1968, and found $R_E = 35 \pm 15 R_\odot$ and $D_E \approx 3 \times 10^{21} cm^2/sec$.

These cosmic ray observations strongly suggest the existence of hydromagnetic waves in the envelope, since such waves are the primary scattering agent at 1 AU (Jokipii, 1971). The gyroradius of a 1 Bev particle near $20 R_\odot$ is $\approx 2 \times 10^4$km and the Alfven speed there is ≈150 km/sec. Assuming that the particles scatter most effectively with wavelengths on the order of the gyroradius, $\lambda \approx R_\odot$, one finds for the characteristic frequency, $\omega \approx 5 \times 10^{-2} sec^{-1}$; this is close to the peak frequency in the observed photospheric and chromospheric acoustic spectrum (Tannenbaum et al. 1969). Burlaga (1970) suggested these might be the waves which Barnes (1968,1969) has considered to be active in heating and accelerating the solar wind.

The technique for remote sensing of the solar envelope which was just described can seldom be applied at 1 AU because of interplanetary fluctuations, but it might be very effective closer to the sun in the region to be explored by the Helios and MVM spacecraft (Figure 1).

B. Acceleration and Heating

1. Acceleration by heating

a). Some basic facts. Observations at 1 AU provide 2 basic results which are essential clues to the acceleration and heating mechanisms: 1) The solar wind speed ranges from ≈250 km/sec to ≈850 km/sec (e.g. see the distribution in Figure 12), and 2) There is a quantitative relation between T_p and V which seems to be valid for all parts of the solar cycle (Burlaga and Ogilvie, 1970a; see Figure 13). The latter result suggest a close relation between the heating and accelerating processes.

Figure 14 compares the various kinds of energy flux and shows how they vary with bulk speed. This is based on the T_p-V relation, on averages of T_e and B, (since these quantities do not change greatly with V - Burlaga and Ogilvie, 1970a, b; Ness et al. 1971; Ogilvie and Scudder, 1971), on the (weak) n-V relation (Burlaga and Ogilvie, 1970 b), and on observations of the heat flux (Montgomery et al., 1968; Ogilvie et al., 1971; Hundhausen and Montgomery, 1971). Clearly the most significant energy flux is that of the flow speed, so it is essential to explain the high speeds that are observed.

b. General Discussion. The problem of accelerating the solar wind to high speeds (up to ≈850 km/sec) is a very old one. Parker (1963) showed that high speeds would result if T were constant out to some distance b $\leq 50 R_\odot$, (Figure 15). Scarf and Noble (1965) pointed out that high speeds are difficult to explain in any other way if the coronal temperature

at $2R_\odot$ is $<2\times10^6$K, as is generally believed. Burlaga and Ogilvie (1970a) showed that Parker's model produces high temperatures at 1 AU as well as high speeds (Table I); the results are consistent with the T_p-V relation within a factor of 2, up to V≈400 km/sec.

If one grants that high speeds are due to an extended region ($\leq50R_\odot$) near the sun where T_p remains near the coronal value, one is faced with the problem of explaining why T_p should remain high. Two mechanisms have been suggested: 1) Protons might receive energy from electrons, which carry energy very efficiently from the sun; 2) Protons might be heated by some external source such as hydromagnetic waves.

Consider the first mechanism. If there is a very strong coupling between the protons and electrons out to $\approx50R_\odot$, then $T_p\approx T_e$ in the envelope. Since $T_e\approx10^6$K out to $\approx30R_\odot$ (Figure 3), one could thereby get the high T_p region suggested by Parker (1963). But what is the nature of the coupling? The Hartle-Sturrock (1968) model shows that such strong coupling is not produced by Coulomb collisions. Hundhausen (1970) argues that there must be some plasma process operating in the envelope which maintains $T_p\approx T_e$. The nature of this process is not known, but Forslund (1970) has discussed some interesting possibilities.

The second mechanism, extended proton heating by an external source, has been reconsidered by Hartle and Barnes (1970) in an effort to explain the T_p-V relation. They show

that if there is an external proton heat source,

$$P_p(r) = D_o\left(\frac{n}{n_o}\right)\exp\left[-\frac{(r/R_\odot - a)}{b}^2\right],$$

then one can explain the T_p-V relation by choosing suitable values of a, b and D_o. They also showed the following general results: a) If energy is deposited below the critical point, the principle result is an increase in V at 1 AU; b) If the energy is deposited above the critical point, the principal result is an increase in T_p; c) If the energy is deposited near the critical point, then both T_p and V are increased. To explain V≈350 km/sec and the corresponding $T_p \approx 5\times10^4$K (Figure 13), Hartle and Barnes (1970) require heating out to $\approx 25R_\odot$ (b=26). Burlaga and Ogilvie (1970a) obtained a similar result from Parker's extended heating model (Table II). Hundhausen (1970) has criticised the introduction of an external heat source on the grounds that the HS model already predicts more energy flux than is observed and by adding another source of energy one just make matters worse. However, the high flux in HS is due to the high conduction flux; one might be able to reduce the heat flux by using a lower K_e, in which case the total flux predicted by Hartle and Barnes would not be unreasonable. Wolfe et al. (1971) have criticised the introduction of an external heat source on the grounds that it is unnecessary since one can explain the observed quiet time conditions using a viscous model with no external heating. However, this model does not explain the higher V, T_p that are more commonly observed, and the importance of viscous heating is still open to question.

Both mechanisms - strong coupling (which gives $T_p=T_e$) and an external heat source (which also gives $T_p \approx T_e$, within a factor of 2 - Figures 3,4)

imply that the solar wind behaves in some respects like a single fluid near the sun. Thus, in either case, a single-fluid model should give a reasonable zeroth order description of the solar wind near the sun. However, the observations that $T_e \neq T_p$ at 1 AU (Figure 13) and that the temperature is anisotropic at 1 AU (Hundhausen, 1968) imply that the solar wind cannot be described as a single-fluid farther from the sun. Indeed, Sturrock and Hartle (1966) actually predicted that $T_p \neq T_e$ before electron measurements were published. Thus, models such as that of Whang (1971a,b) with one-fluid out to $b \approx 50 R_\odot$ and 2-fluids beyond appear to be more appropriate than 1-fluid models.

b). Heating by Wave Damping. The Hartle and Barnes (1970) model, which postulates an external heat source, does not specify the physical nature of the source. Barnes et al. (1971) suggested that the heating mechanism is the collisionless damping of fast mode hydromagnetic waves propagating from the sun into the region of increasing β (Figure 5). Introducing a variable iostropic flux F_o of such waves with frequency $\omega_o = .02$ sec^{-1} into the 2-fluid model of Hartle and Sturrock (1968) they found that the T-V relation is actually "predicted" by the model (Figure 16). Higher speeds and temperatures are obtained by increasing a single parameter, F_o. Most of the wave energy is deposited within $20 R_\odot$ (Figure 17).

Is there enough wave energy available to give the observed speeds? The model requires $F_o = 6.5 \times 10^3$ erg/cm^{2}sec at $2 R_\odot$ to produce V=390 km/sec. This implies an efflux of $\approx 10^{27}$ erg/sec which is less than the power required to heat the inner corona (5×10^{27} ergs/sec) and the chromosphere (5×10^{29} erg/sec).

The model predicts that B should be nearly independent of V, in

agreement with observations (Burlaga and Ogilvie, 1970b) and that T_e should decrease somewhat with increasing V. However, the densities and thus the total energy flux are somewhat high, especially at high speeds, and B is too low at all speeds. Perhaps time variations and departures from spherical symmetry must be considered to explain these discrepancies. The model also predicts a high T_e because it uses the Chapman conductivity.

Finally, the model does not include Maxwell stresses due to the background magnetic field. Since the energy in the magnetic fluctuations is only a fraction of that in the background field, it is not clear that the neglect of the latter is justified particularly where B>1G at the sun (Whang, private communication).

2. Acceleration by Waves in the Envelope.

We have seen how fast waves might accelerate the solar wind by damping. Alazraki and Couturier (1971) and Belcher (1971) have shown that Alfven waves propagating from the sun might accelerate the solar wind directly if they are not damped.

The Poynting flux of Alfven waves is

$$F_w = 4\pi r^2 \frac{B^2}{4\pi} \epsilon (V+V_A)$$

where $\epsilon = (\delta B)^2/2B^2)$ and δB is the wave amplitude. This can be very large near the sun because V_A is large there (Figure 7). For example, at $r_o=10^6$km $F_w \approx \epsilon B_o^2 V_A r_o^2 = \epsilon\ 5\times10^{29}$erg/sec which is comparable to the total flow energy at 1 AU (10^{27}erg/sec, Figure 14) even if ϵ is as small as 1/50.

Belcher used a 1-fluid, polytrope model to study the effect of such wave fluxes. Two solutions, for ϵ=0 and for ϵ=.01, are shown in Figure 18. Very low speeds at 1 AU (V≈150 km/sec) are obtained with ϵ=0,

but much higher speeds ($V \approx 360$ km/sec) are obtained with even small amplitude waves ($\epsilon = .01$). Most of the acceleration occurs close to the sun (Figure 18.).

This model neglects damping, uses the WKB approximation, and assumes strong coupling between electrons and protons. A more realistic 2-fluid model with Alfven wave damping is currently being constructed by Barnes and others.

3. Acceleration by $\underset{\sim}{B}$.

Whang (1971a) has shown that the transformation of magnetic energy into kinetic energy during the expansion process might cause a small (~17%) increase in the solar wind speed at 1 AU at quiet times if $B(r_\odot) = 2G$. Thus, including $\underset{\sim}{B}$ in a model such as that of Hartle and Sturrock (1968) could increase V from 250 km/sec to ≈300 km/sec.

In Whang's model the acceleration is caused by the Lorentz force

$$\frac{1}{c} \underset{\sim}{J} \times \underset{\sim}{B} = \frac{B^2}{4\pi V} \sin^2 \varphi \frac{dV}{dr}$$

which is everywhere positive, directed away from the sun; here φ is the angle between $\underset{\sim}{B}$ and the radial direction. The acceleration results from the fact that near the sun the smallest φ given by Whang's solution, is 3.5^o.

The process can also be viewed as one of energy conversion. There is a non-zero component of the Poynting flux

$$P_r = \frac{VB^2 \sin^2 \varphi}{4\pi} \propto \frac{1}{r^2 V(r)} .$$

Since the total energy flux is constant, the loss of Poynting flux ultimately appears as kinetic energy of the wind. Whang finds that 90% of the Poynting energy is deposited with $10R_\odot$ (See Figure 19).

C. Angular Momentum

The flux of angular momentum is related to the Maxwell stress by the equation

$$(\rho V_\varphi r)V - \frac{rB_r B_\phi}{4\pi} = \rho VL$$

where V_φ is the azimuthal wind speed and L is a constant. With the frozen field condition and the equations $\nabla \times E = \nabla \cdot B = 0$, this gives

$$r(VB_\varphi - V_\phi B_r) = -r^2 \Omega B_r = \text{const}$$

Thus, $$V_\varphi = r\Omega\left[\frac{M_A^2 L}{\Omega r^2} - 1\right]/(M_A^2 - 1)$$

where $M_A = V/V_A$. To avoid a singularity at $M_A = 1$ (the Alfven critical point), one must set $L = \Omega r_A^2$, where r_A is the point at which $M_A = 1$ ($\approx 25 R_\odot$). Weber and Davis (1967) find that V_φ increases to a maximum $V_{\varphi max} = 3.8$ km/sec at $11.5 R_\odot$ and then decreases to ≈ 1 km/sec 1 AU. Thus, the effect of the magnetic torque is largest in the envelope, at $\approx 10 R_\odot$, and is very small at 1 AU. Similar results were found by Brandt et al. (1969).

Weber and Davis (1970) have also considered the effect of mechanical stresses on V_φ. The basic equation in this case is

$$(\rho V_\varphi r)\, V = r(\sigma^o_{r\varphi} - p_{r\varphi} + \frac{B_r B_\varphi}{4\pi}) + \text{constant},$$

where $\sigma^o_{r\varphi}$ is the viscous stress and $p_{r\varphi}$ is the stress due to anisotropy. Using the Chapman formula for viscosity and assuming a rather high proton temperature at earth, $T \approx 2 \times 10^5$ K (which greatly increases the effect of viscosity, since $\eta \propto T_p^{5/2}$), Weber and Davis (1970) found that the viscous term is dominant outside the envelope and can give V_φ as large as 6 km/sec at 1 AU. On the other hand, using a similar model which neglects $p_{r\varphi}$ and assumes a lower T_p

at 1 AU ($T_p \approx 4 \times 10^4$ K), Wolff et al. (1971) found a much lower speed at 1 AU (V_φ=1.8 km/sec), which is comparable to that caused by the Maxwell stress alone (Weber and Davis, 1967; Brandt et al. 1969). Their curve for $V_\varphi(r)$, is shown in Figure 20. Of course, if Parker's comments on viscosity are correct, the effects of viscosity are negligible, and the magnitude of V_φ in Figure 20 should be reduced by a factor of 2.

The observations of V_φ are still in a rather confused state. Experimental data for V_φ at 1 AU range from -1.5 km/sec to 10 km/sec. (Brandt and Heise, 1970; Coon, 1969; Egidi et al., 1969; Strong et al., 1968). Apart from the instrumental problems of measuring V_φ, there are difficulties due to the fluctuations in V_φ caused by stream interactions, (Lazarus and Goldstein, 1971; Siscoe, 1971; Carovillano and Siscoe, 1969) hydromagnetic waves (Belcher and Davis 1971) and other factors not yet understood. Thus, the angular momentum flux can best be studied by going close to the envelope or into the envelope where V_φ is largest and V_r is smaller.

IV. Discussion

Although it is necessary to use some controversial models to extrapolate to conditions near the sun, it is clear that the region within $25R_{\odot}$ (the solar envelope) is very different from the interplanetary medium and that characteristics of the solar wind at 1 AU are largely determined by processes in the envelope.

The magnetic field rules in the envelope: The Alfven speed is larger than the sound speed; the magnetic energy density is larger than the thermal energy density and the flow energy density; hydromagnetic waves may be propagating away from the sun, possibly scattering cosmic rays; hydromagnetic waves will damp, thereby heating and accelerating the solar wind; the Lorentz force might accelerate the solar wind to some extent; and the magnetic field causes the plasma to corotate. Dynamical effects due to stream interactions are probably small near the envelope.

The experimental study of the envelope is of considerable importance, but it will remain inaccessible to direct probes for many years. In the meantime, the Helios and MVM spacecraft will approach the edge of the envelope and it will be possible to study of the envelope remotely by means of cosmic rays, MHD, waves etc., free of complications due to interplanetary effects.

TABLE I

$b\ (\times 10^6\ km)$	$V\ (km/sec)$	$T\ (\times 10^4\ °K)$	$T\ (OBSERVED)\ (\times 10^4\ °K)$
5.4	260	0.6	1.2
8	320	1.2	3.6
20	410	5.0	8.5
40	460	14.0	13.0

ACKNOWLEDGEMENTS

The author is indebted to Drs. Brandt, Hartle, Hundhausen, Schatten, and Whang for stimulating discussions and helpful suggestions. Mr. D. Stief prepared several figures.

FIGURE CAPTIONS

Figure 1 Solar envelope. This shows the size and location of the envelope in relation to other parts of the sun's "atmosphere".

Figure 2 "Quiet-time" model of n(r) and B(r).

Figure 3 "Quiet-time" proton temperature profiles. Two models are shown. One (HB) is a non-viscous model with proton heating out to $\approx 25\ R_\odot$. The other (WB) is a viscous model with $T=T_e$ out to $3R_\odot$.

Figure 4 Electron temperature profiles.

Figure 5 $\beta(r)$

Figure 6 Flow energy density and internal energy density versus r.

Figure 7 Characteristic speeds in the solar wind. The numbers are estimates which may be in error by a factor of 2.

Figure 8 Stream interaction in a steady wind due to a sinusoidal variation in $V_r(\varphi)$ at $10R_\odot$.

Figure 9 Stream interaction due to the time varying, spherically symmetric heat source at .1 AU shown in the insert.

Figure 10 Distribution of positive and negative ΔV the difference between consecutive 3-hour averages of the bulk speed.

Figure 11 May 4, 1960, cosmic ray event. Observations are shown as points. The solid line is a theoretical curve.

Figure 12 Distribution of speeds. This particular distribution of speeds is based on Explorer 34 data for the period June - December, 1967.

Figure 13 T_p-V relation. Explorer 34 data for 1967 (open circles) show a relation between the proton temperature and speed. Data from other parts of the solar cycle fall on the same line,

indicating that the T_p-V relation is a very general property of the solar wind. The 2-fluid model of Hartle and Barnes gives a point which is close to the T_p-V curve. Electron observations suggest that T_e is nearly independent of V, as indicated.

Figure 14 Relative sizes of various energy fluxes versus V.

Figure 15 The observed range of wind speeds can be explained by extended heating region. The model shown here assumes an isothermal region of radius b followed by a region where the wind cools adiabatically.

Figure 16 The T_p-V relation predicted by damping of a variable flux F_o of fast-mode waves, compared with the observed T-V relation.

Figure 17 Most fast-mode wave energy is deposited in the envelope.

Figure 18 V(r) predicted by a polytrope model with (ϵ=0) Alfven waves. Alfven waves can cause significant acceleration in the envelope.

Figure 19 Most of the Poynting energy due to a steady $\underset{\sim}{B}$ is deposited near the sun.

Figure 20 $V_\varphi(r)$, assuming both magnetic stresses and viscosity.

REFERENCES

Alazraki, G., and P. Couturier, Solar wind acceleration caused by the gradient of Alfven wave pressure, Astron. and Astrophys., 13, 380, 1971.

Barnes, A., Collisionless heating of the solar wind plasma I. Theory of the heating of collisionless plasma by hydromagnetic waves. Astrophys. J., 154, 751, 1968.

Barnes, A., Collisionless heating of the solar wind plasma II. Application of the theory of plasma heating by hydromagnetic waves. Astrophys. J., 155, 311, 1969.

Barnes, A., R. E. Hartle, and J. H. Bredekamp, On the energy transport in stellar winds, Astrophys. J. Letters, 166, L53, 1971.

Belcher, J. W., and L. Davis, Jr., Large-amplitude Alfven waves in the interplanetary medium, 2, J. Geophys. Res., 76, 3534, 1971.

Belcher, J. W., Alfvenic wave pressures and the solar wind, Astrophys. J., (to be published) 1971.

Brandt, J. C., and J. Heise, Interplanetary gas XV. Nonradial plasma motions from the orientations of ionic comet tails, Astrophys. J., 159, 1057, 1970.

Brandt, J. C., C. L. Wolff, and J. P. Cassinelli, Interplanetary gas XVI. A calculation of the angular momentum of the solar wind, Astrophys. J., 156, 1117, 1969.

Braginskii, S. I., Transport processes in a plasma, Rev. Plasma Phys., 1, 205, 1965.

Burlaga, L. F., Anisotropic cosmic ray propagation in an inhomogeneous medium I. The solar envelope, In Proc. 11th Int. Conf. on Cosmic Rays, Budapest 1969, Acta Physica Academiae Scientiarum Hungaricae 29 Suppl. 2,9, 1970.

Burlaga, L. F., and K. W. Ogilvie, Heating of the Solar wind, Astrophys. J., 159, 659, 1970a.

Burlaga, L. F., and K. W. Ogilvie, Magnetic and thermal pressures in the solar wind, Solar Physics, 15, 61, 1970b.

Burlaga, L. F., K. W. Ogilvie, D. H. Fairfield, M. D. Montgomery, and S. J. Bame, Energy transfer at colliding streams in the solar wind, Astrophys. J., in press, 1971.

Carovillano, R. L., and G. L. Siscoe, Corotating structure in the solar wind, Solar Physics, 9, 1969.

Coon, J. H., in Earth's Particles and Fields, p.359, ed. by B. M. McCormac, Reinhold Book Corporation, New York, 1969.

Duggal, S. P., M. A. Pomerantz, and I. Guidi, The unusual anisotropic solar particle event of November 18, 1968, (to be published) 1971.

Egidi, A., C. Passella, and C. Signorini, Measurement of the solar wind direction with the IMP I satellite, J. Geophys. Res., 74, 2807, 1969.

Fisk, L. A., and K. H. Schatten, Transport of cosmic rays in the solar corona, NASA-GSFC X-661-71-313, to appear in Solar Physics, 1971.

Formiso, V., and J. K. Chao, On the generation of shock pairs in the solar wind, to be published, 1971.

Forslund, D. W., Instabilities associated with heat conduction in the solar wind and their consequences, J. Geophys. Res., 75, 17, 1970.

Goldstein, B. E., Non-linear corotating solar wind structure (to be published) 1971.

Gosling, J. T., and S. J. Bame, Solar wind speed variations 1964-1967: An autocorrelation Analysis, (to be published) 1971.

Hartle, R. E., and A. Barnes, Nonthermal heating in the two-fluid solar wind model, J. Geophys. Res., 75, 6915, 1970.

Hartle, R. E., and P. S. Sturrock, Two-fluid model of the solar wind, Astrophys. J., 151, 1155, 1968.

Hundhausen, A. J., Direct observations of solar wind particles, Space Sci. Rev., 8, 690, 1968.

Hundhausen, A. J., Nonthermal heating in the solar wind, J. Geophys. Res., 74, 5810, 1969.

Hundhausen, A. J., Composition and dynamics of solar wind plasma, Rev. Geophys. and Space Phys., 8, 729, 1970.

Hundhausen, A. J., and R. A. Gentry, Numerical simulation of flare-generaged disturbances in the solar wind, J. Geophys. Res., 74, 2908, 1969.

Hundhausen, A. J., and M. D. Montgomery, Heat conduction and non-steacy phenomena in the solar wind, J. Geophys. Res., 76, 2236, 1971.

Jokipii, J. R., Propagation of solar flare cosmic rays in the solar wind, Rev. Geophys. Space Phys., 9, 27, 1971.

Lazarus, A. J., and B. E. Goldstein, Observation of the angular momentum flux carried by the solar wind, J. Geophys. Res., (to be published) 1971.

Lust, R., and J. A. Simpson, Initial stages in the propagation of cosmic rays produced by solar flares, Phys. Rev., 108, 1536, 1957.

McCracken, K. G., The cosmic ray flare effect 3. Deductions regarding the interplanetary magnetic field, J. Geophys. Res., 67, 447, 1962.

Meyer, P., E. N. Parker, and J. A. Simpson, Solar cosmic rays of February, 1956 and their propagation through interplanetary space, Phys. Rev., 104, 768, 1956.

Montgomery, M. D., S. J. Bame, and A. J. Hundhausen, Solar wind electrons: Vela 4 measurements, J. Geophys. Res., 73, 4999, 1968.

Ness, N. F., A. J. Hundhausen, and S. J. Bame, Observations of the interplanetary medium: Vela 3 and IMP 3 1965-1967, J. Geophys. Res., (in press, 1971).

Neugebauer, M. and C. W. Snyder, Mariner 2 observations of the solar wind 1. Average properties, J. Geophys. Res., 71, 4469, 1966.

Ogilvie, K. W., J. D. Scudder, and M. Sugiura, Electron energy flux in the solar wind, J. Geophys. Res., (in press) 1971.

Parker, E. N., Interplanetary dynamical processes, John Wiley, New York, 1963.

Parker, E. N., Dynamical theory of the solar wind, Space Sci. Rev., 4, 666, 1965.

Scarf, F. L., and L. M. Noble, Conductive heating of the solar wind II. The inner corona, Astrophys. J., 141, 1479, 1965.

Schatten, K. H., Evidence for a coronal magnetic bottle at 10 solar radii, Solar Physics, 12, 484, 1970.

Siscoe, G. L., Structure and orientations of solar wind interaction fronts: Pioneer 6, to appear in J. Geophys. Res., 1971.

Strong, J. B., J. R. Asbridge, S. J. Bame, and A. Hundhausen, in the Zodiacal Light and the Interplanetary Medium, ed. J. L. Weinberg (Washington NASA SP-150) p.365, 1968.

Sturrock, P. A., and R. E. Hartle, Two-fluid model of the solar wind, Phys. Rev. Letters, 16, 628, 1966.

Tannenbaum, A. S., J. M. Wilcox, E. N. Frazier, and R. Howard, Solar velocity fields: 5-min. oscillations and super granulation, Solar Physics, 9, 328, 1969.

Weber, E. J., and L. Davis, Jr., The angular momentum of the solar wind, Astrophys. J., 148, 217, 1967.

Weber, E. J., and L. Davis, Jr., The effect of viscosity and anisotropy in the pressure on the ezimuthal motion of the solar wind, J. Geophys. Res., 75, 2419, 1970.

Whang, Y. C., Conversion of magnetic field energy into kinetic energy in the solar wind, Astrophys. J., (to appear) 1971a.

Whang, Y. C., Higher moment equations and the distribution function of the solar wind plasma, to be published in J. Geophys. Res., 1971b.

Wolff, C. L., J. C. Brandt, and R. G. Southwick, A two-component model of the quiet solar wind with viscosity, magnetic field, and reduced heat conduction, Astrophys. J., 165, 181. 1971.

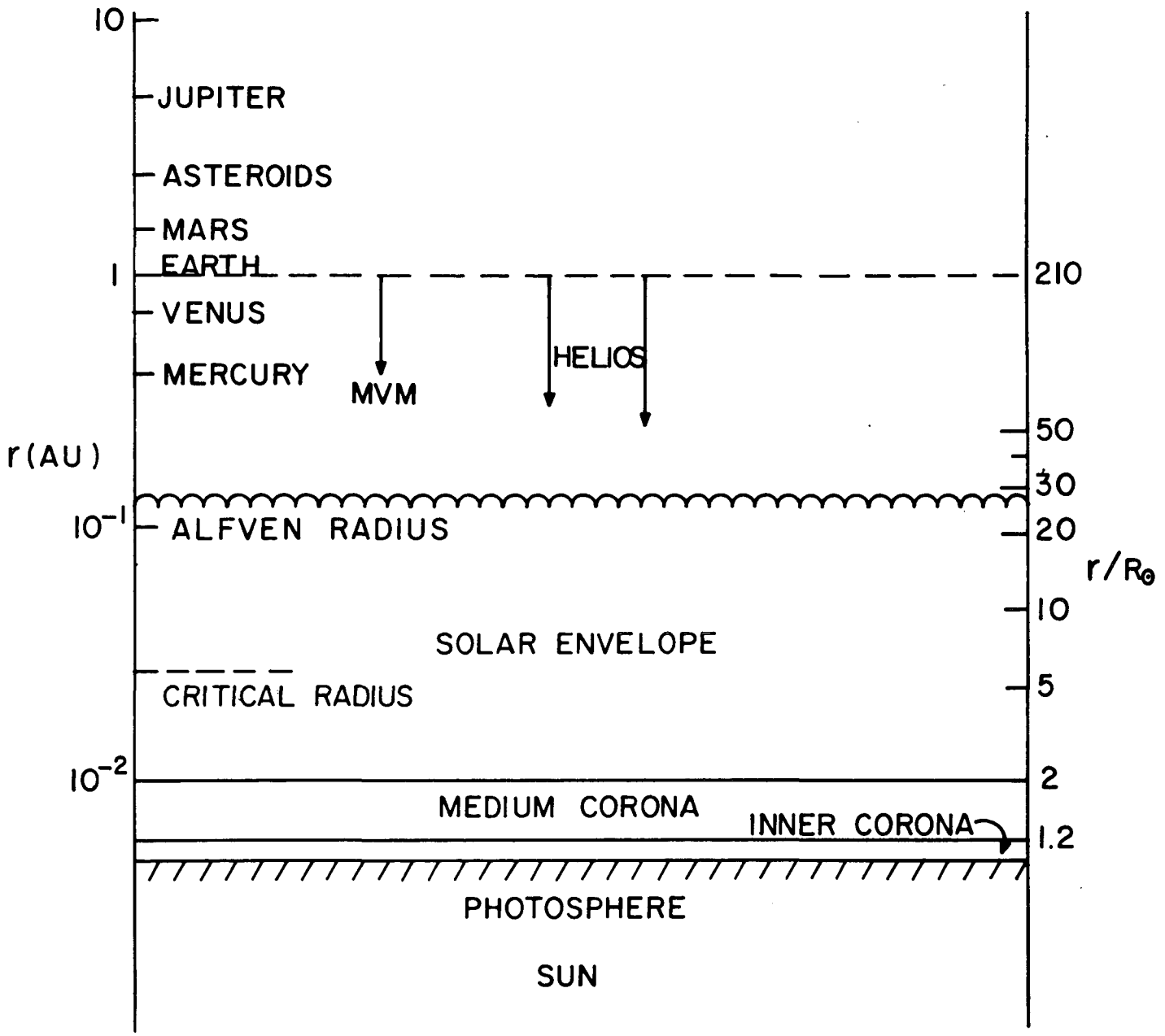
10
JUPITER
ASTEROIDS
MARS
EARTH
1
VENUS
MERCURY
MVM
HELIOS
r(AU)
10^{-1}
ALFVEN RADIUS
SOLAR ENVELOPE
CRITICAL RADIUS
10^{-2}
MEDIUM CORONA
INNER CORONA
PHOTOSPHERE
SUN
210
50
30
20
10
5
2
1.2
$r/R_\odot$

Figure 1

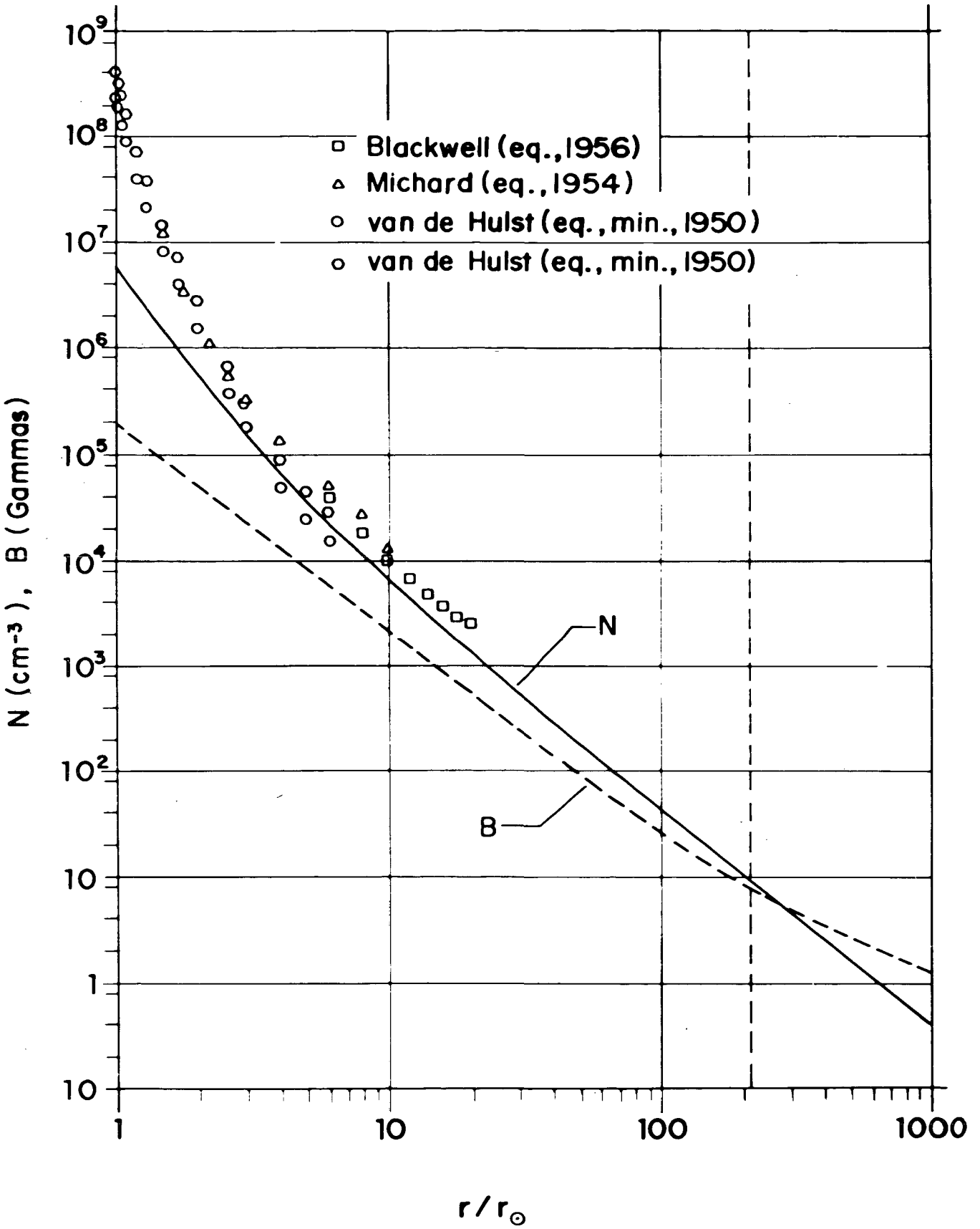
Blackwell (eq., 1956)
Michard (eq., 1954)
van de Hulst (eq., min., 1950)
van de Hulst (eq., min., 1950)
N
B
N (cm⁻³), B (Gammas)
r/r⊙
10⁹
10⁸
10⁷
10⁶
10⁵
10⁴
10³
10²
10
1
10
1
10
100
1000

Figure 2

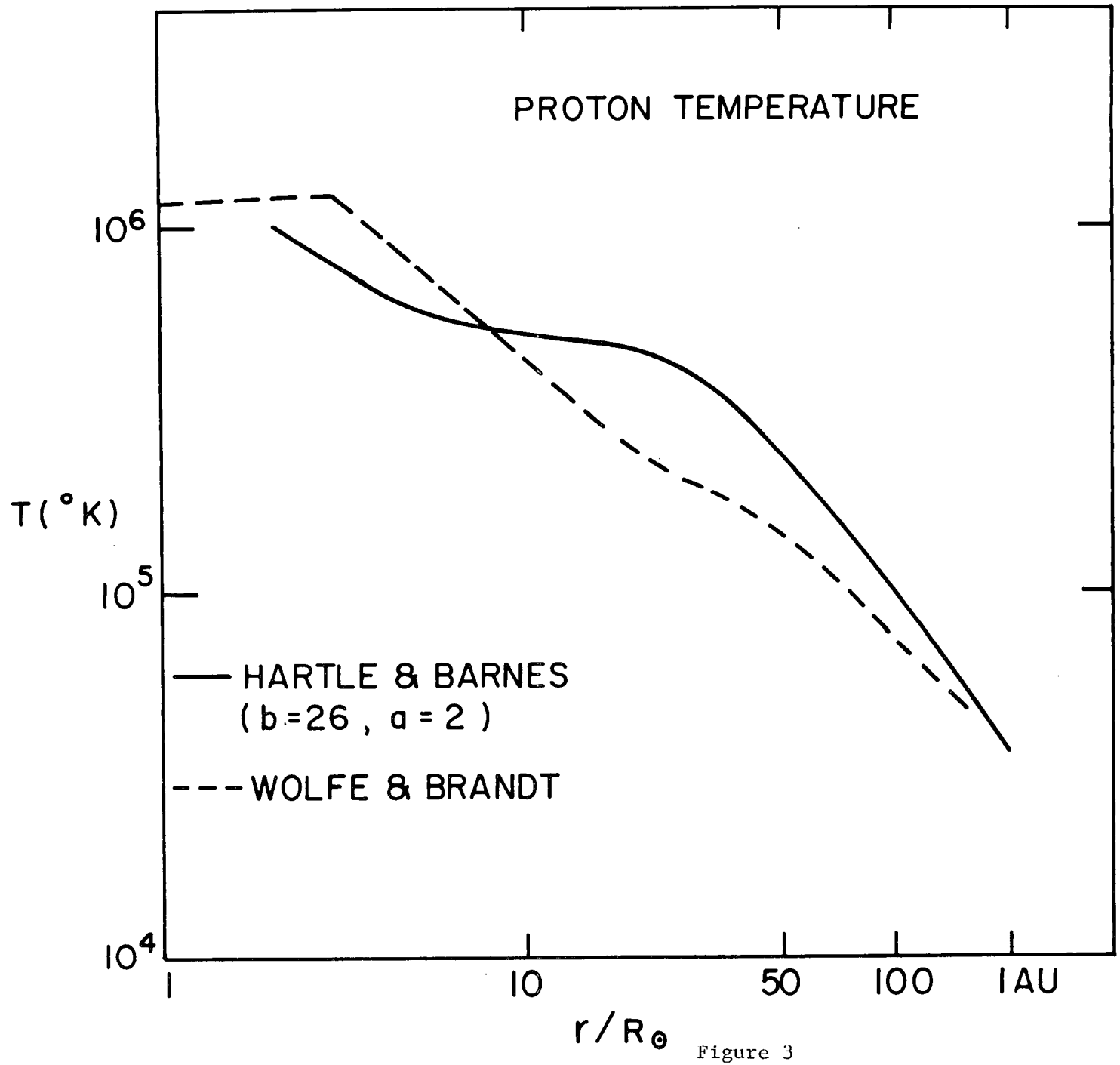
PROTON TEMPERATURE
10^6
10^5
10^4
T(°K)
HARTLE & BARNES
(b=26, a=2)
WOLFE & BRANDT
1
10
50
100
1AU
$r/R_\odot$

Figure 3

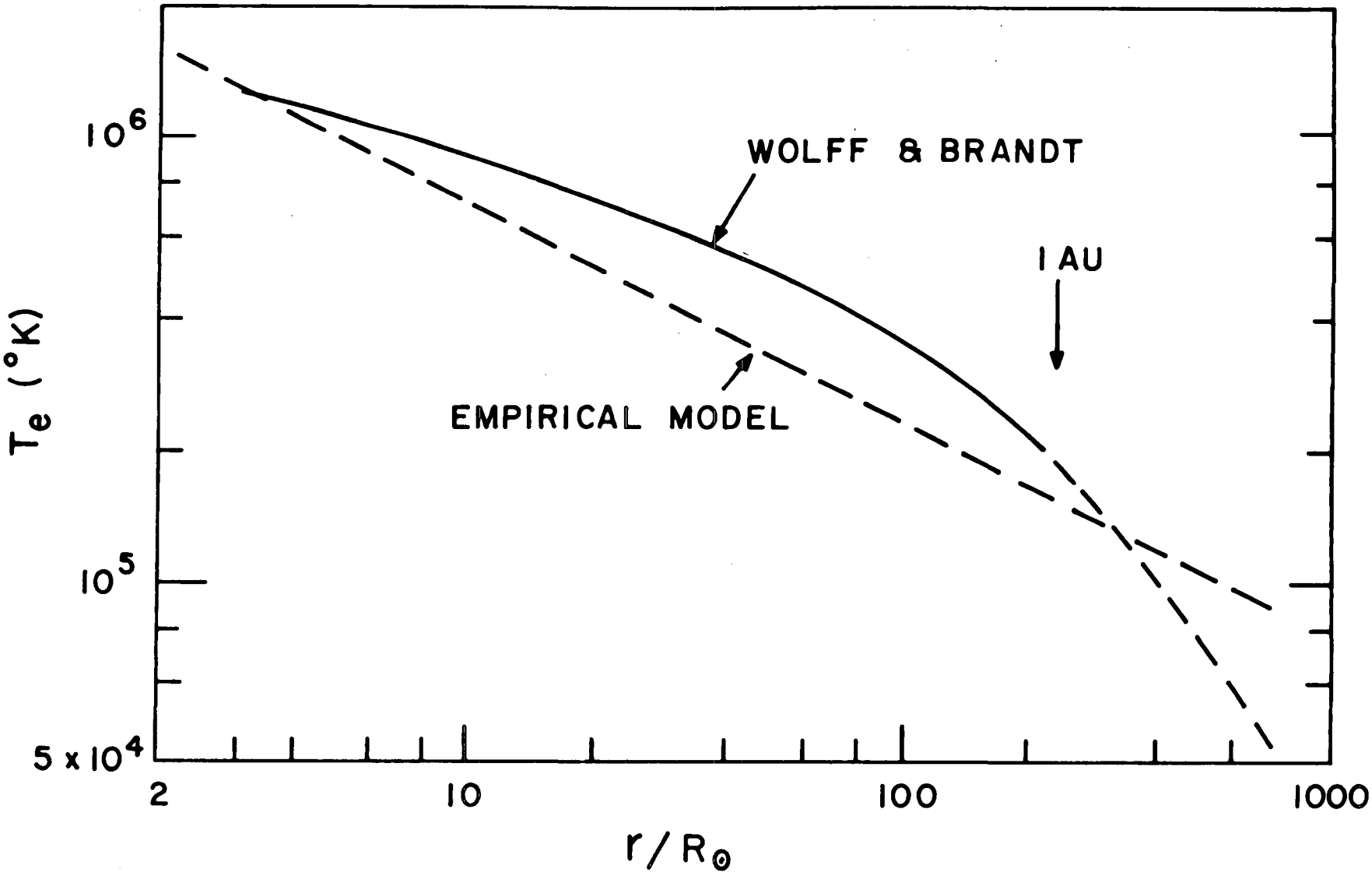
WOLFF & BRANDT
1 AU
EMPIRICAL MODEL
T_e (°K)
10^6
10^5
5×10^4
2
10
100
1000
$r/R_\odot$

Figure 4

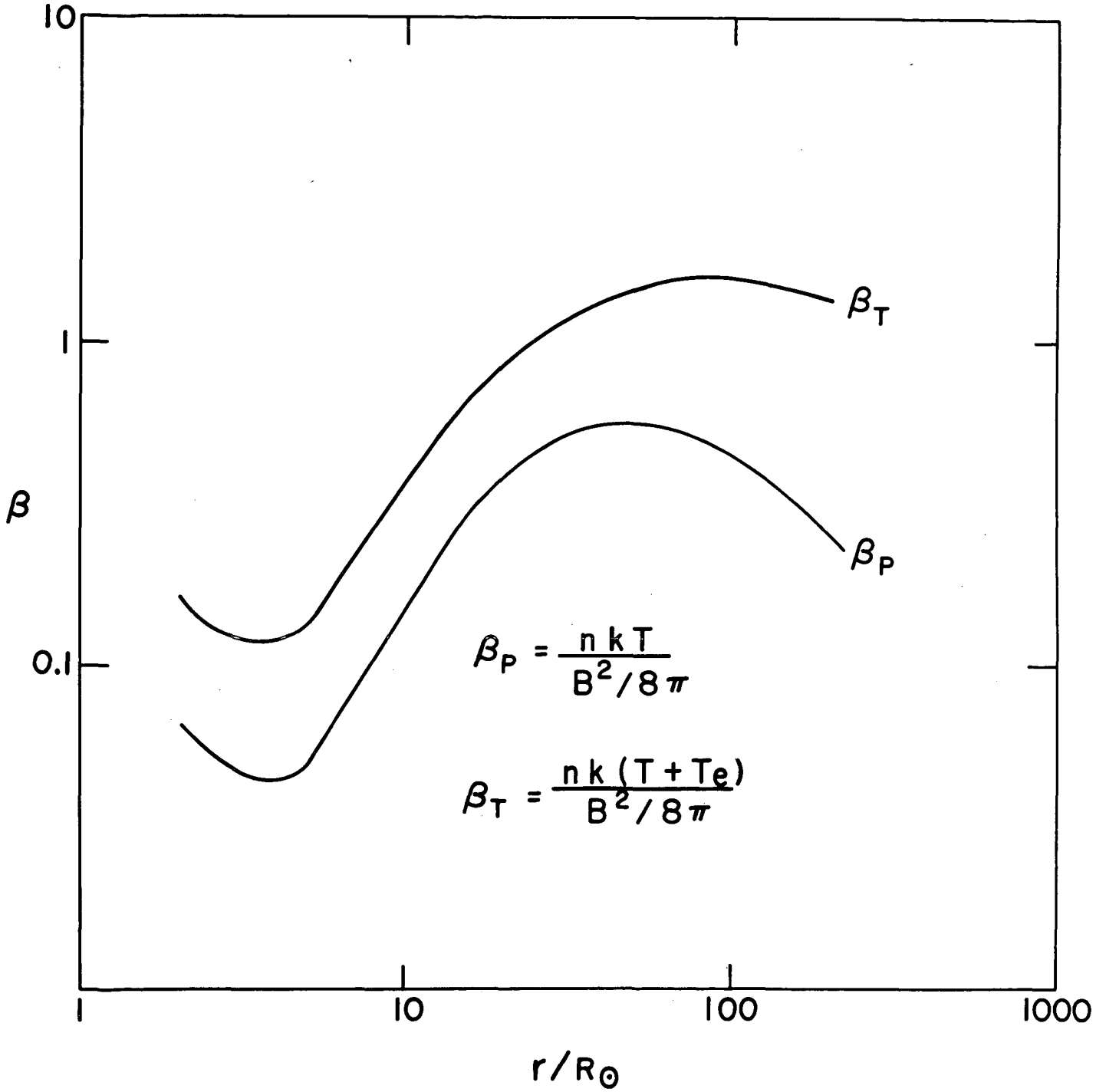
10
1
0.1
β
β_T
β_P
$\beta_P = \frac{n k T}{B^2/8\pi}$
$\beta_T = \frac{n k (T + Te)}{B^2/8\pi}$
1
10
100
1000
$r/R_\odot$

Figure 5

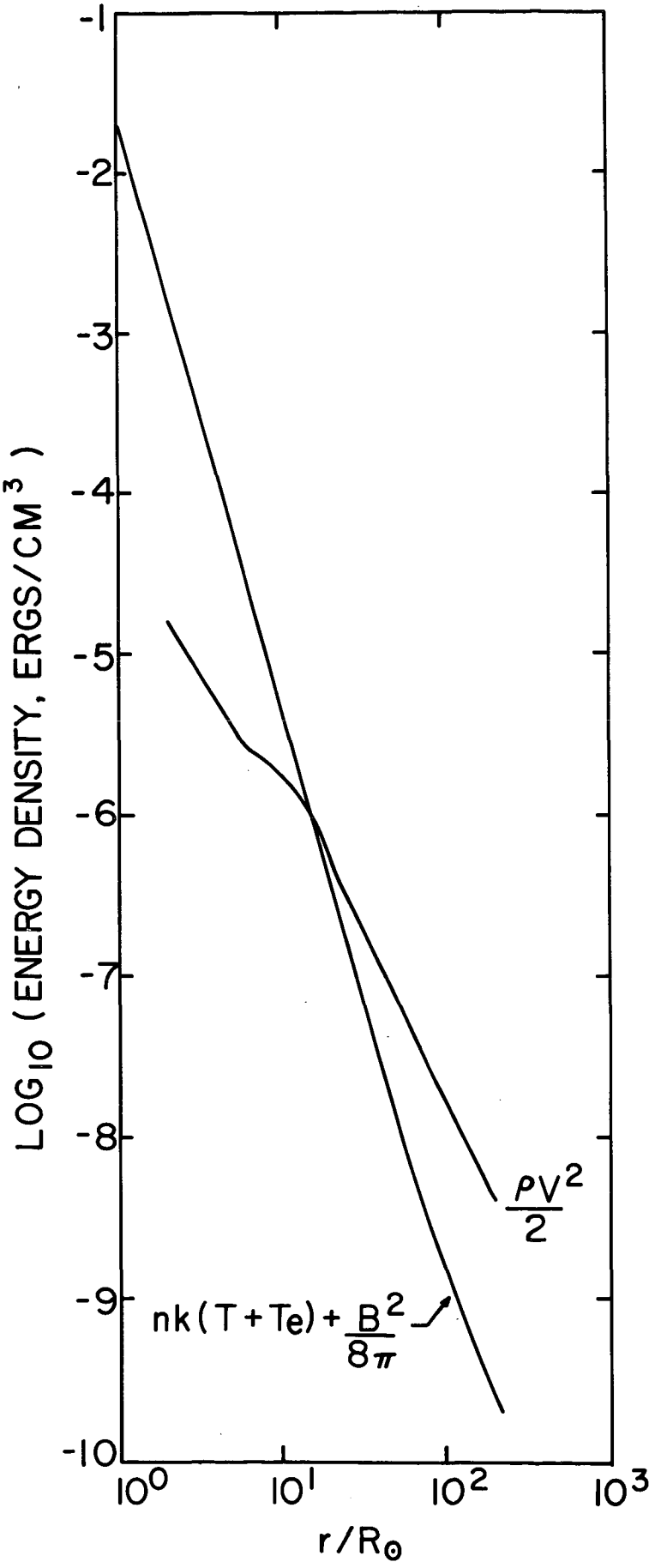
-1
-2
-3
-4
-5
-6
-7
-8
-9
-10
LOG10 (ENERGY DENSITY, ERGS/CM3)
ρV2/2
nk(T+Te)+B2/8π
10^0
10^1
10^2
10^3
r/R⊙

Figure 6

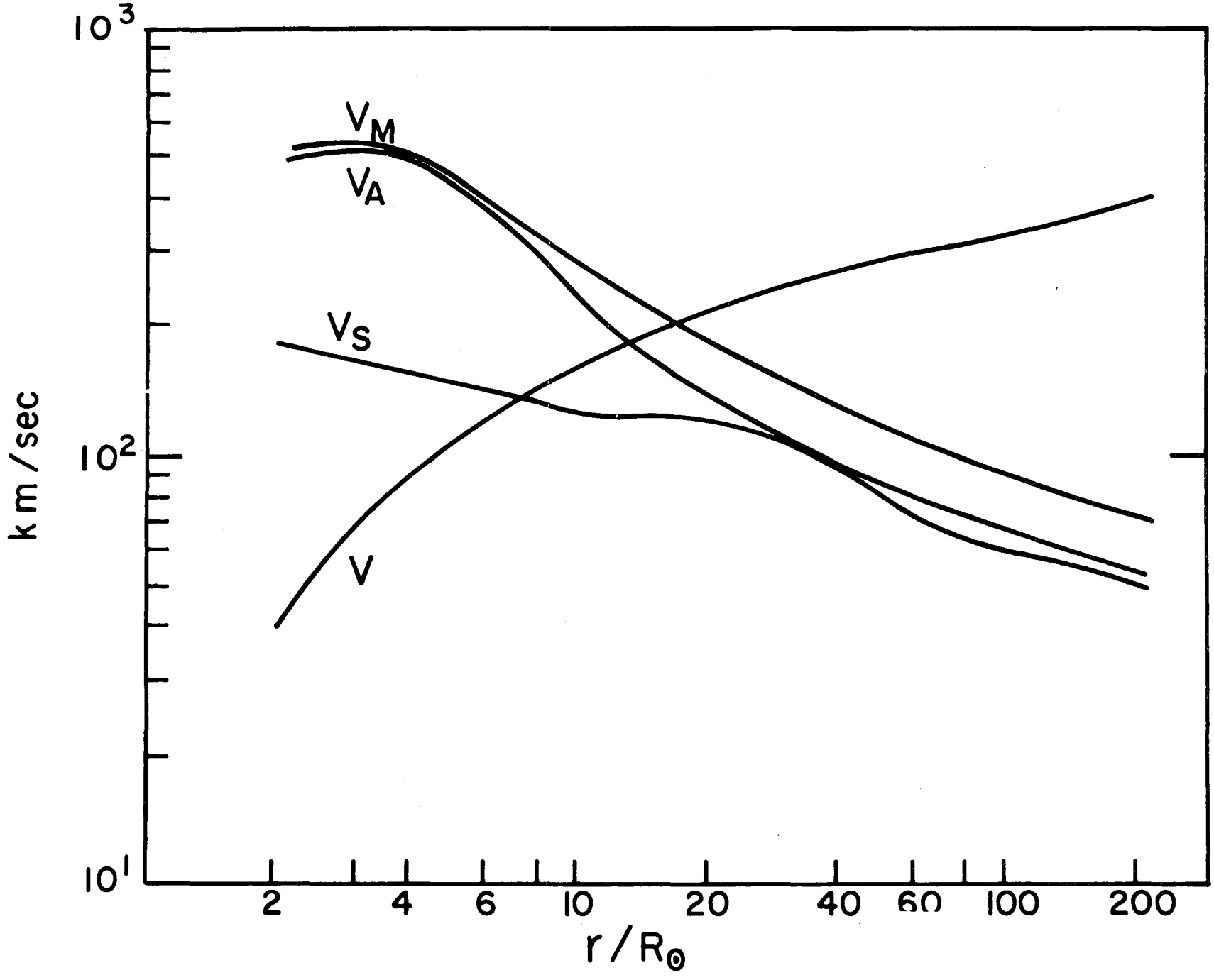

Figure 7

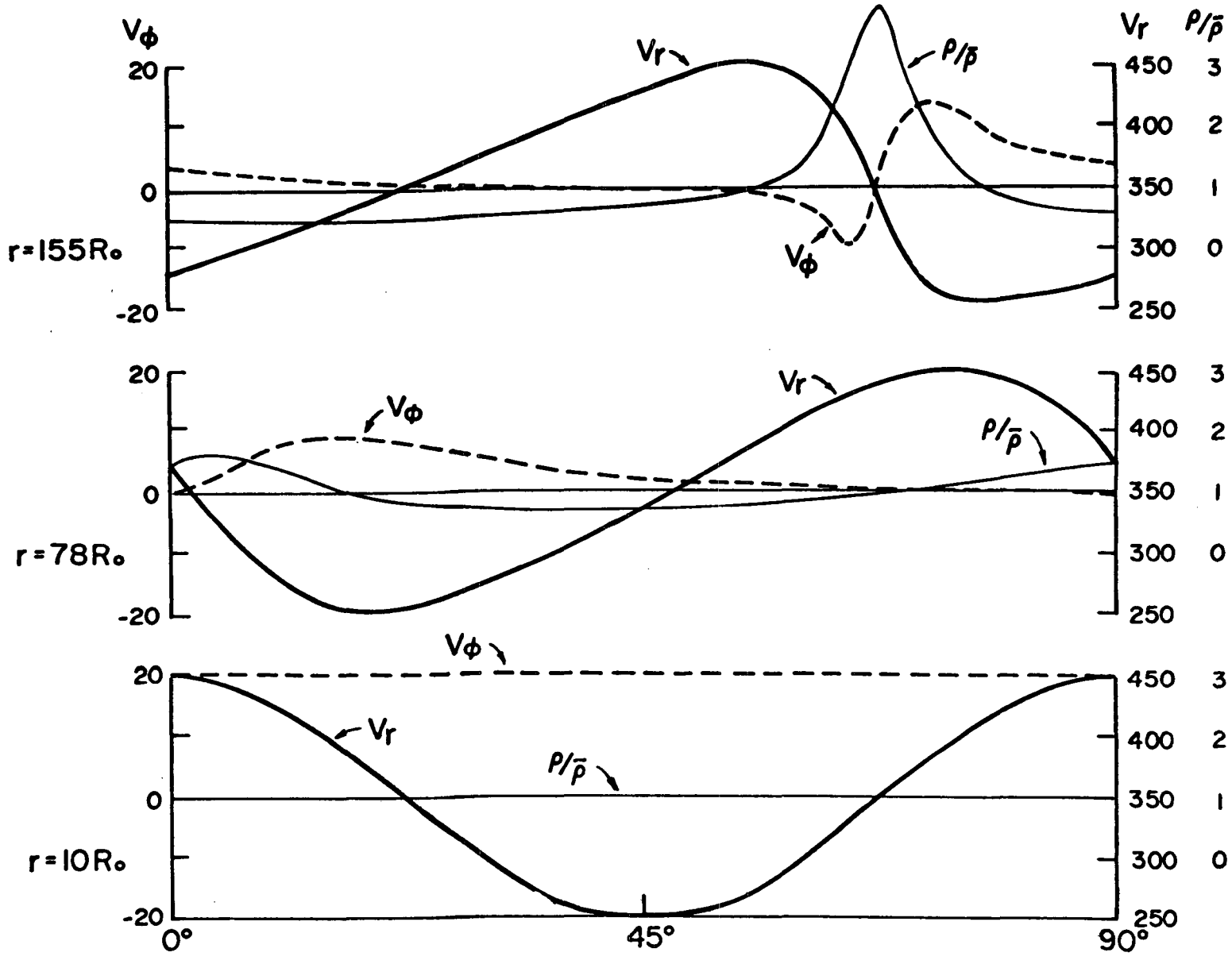
Vφ
Vr
ρ/ρ̄
20
0
-20
r=155Ro
450
400
350
300
250
3
2
1
0
r=78Ro
r=10Ro
0°
45°
90°

Figure 8

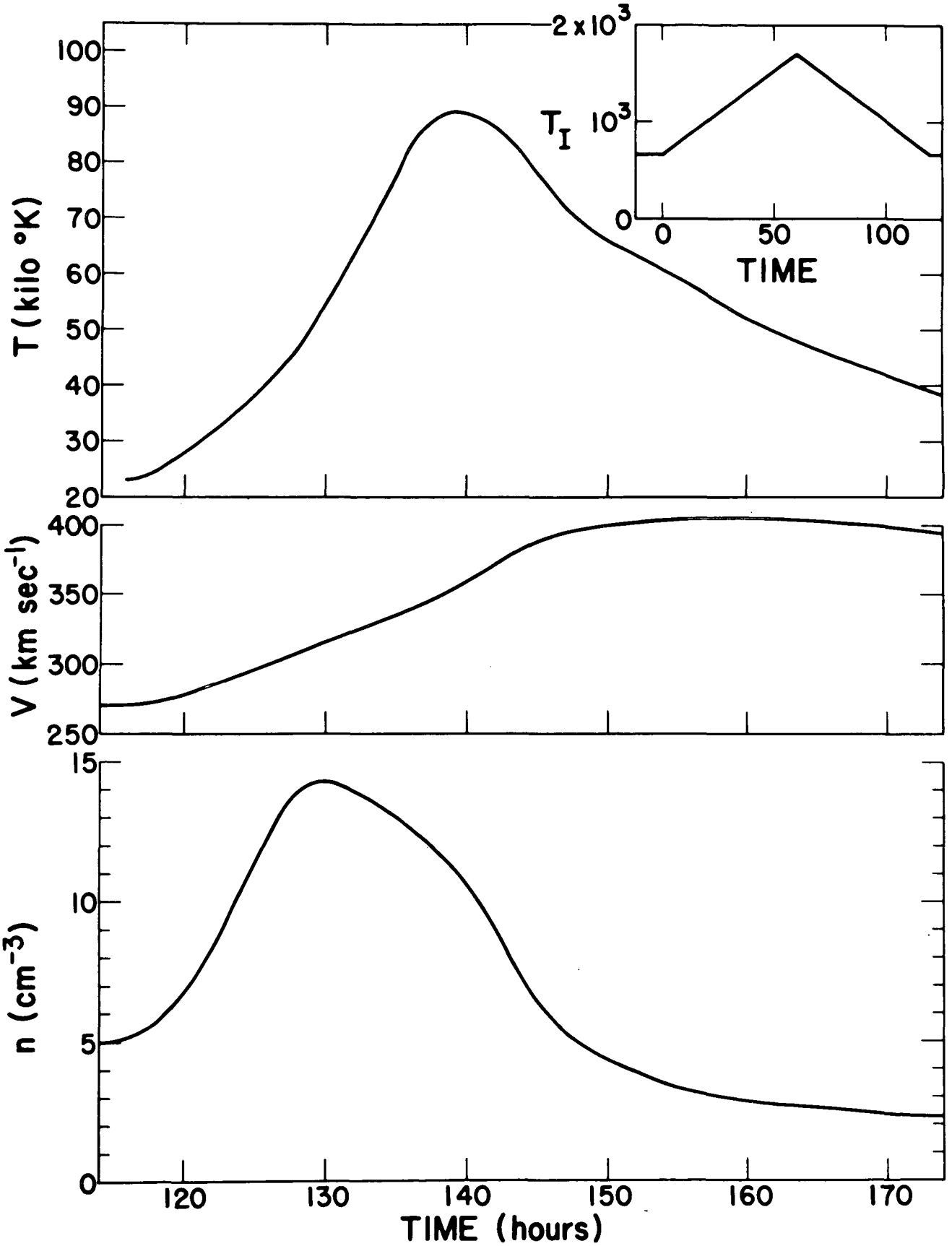
2 x 10^3
T_I
10^3
0
0
50
100
TIME
T (kilo °K)
100
90
80
70
60
50
40
30
20
V (km sec^-1)
400
350
300
250
n (cm^-3)
15
10
5
0
120
130
140
150
160
170
TIME (hours)

Figure 9

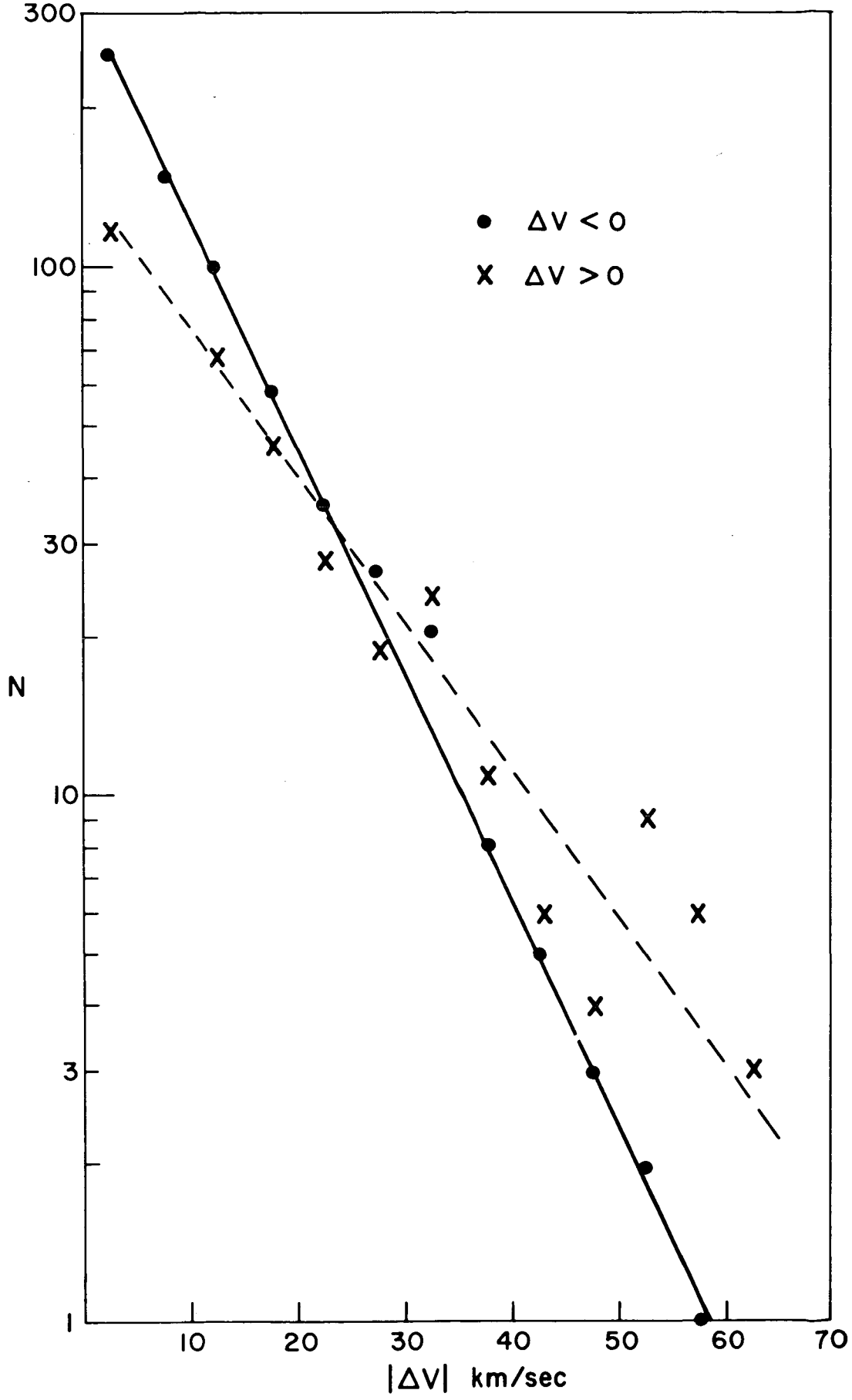

Figure 10

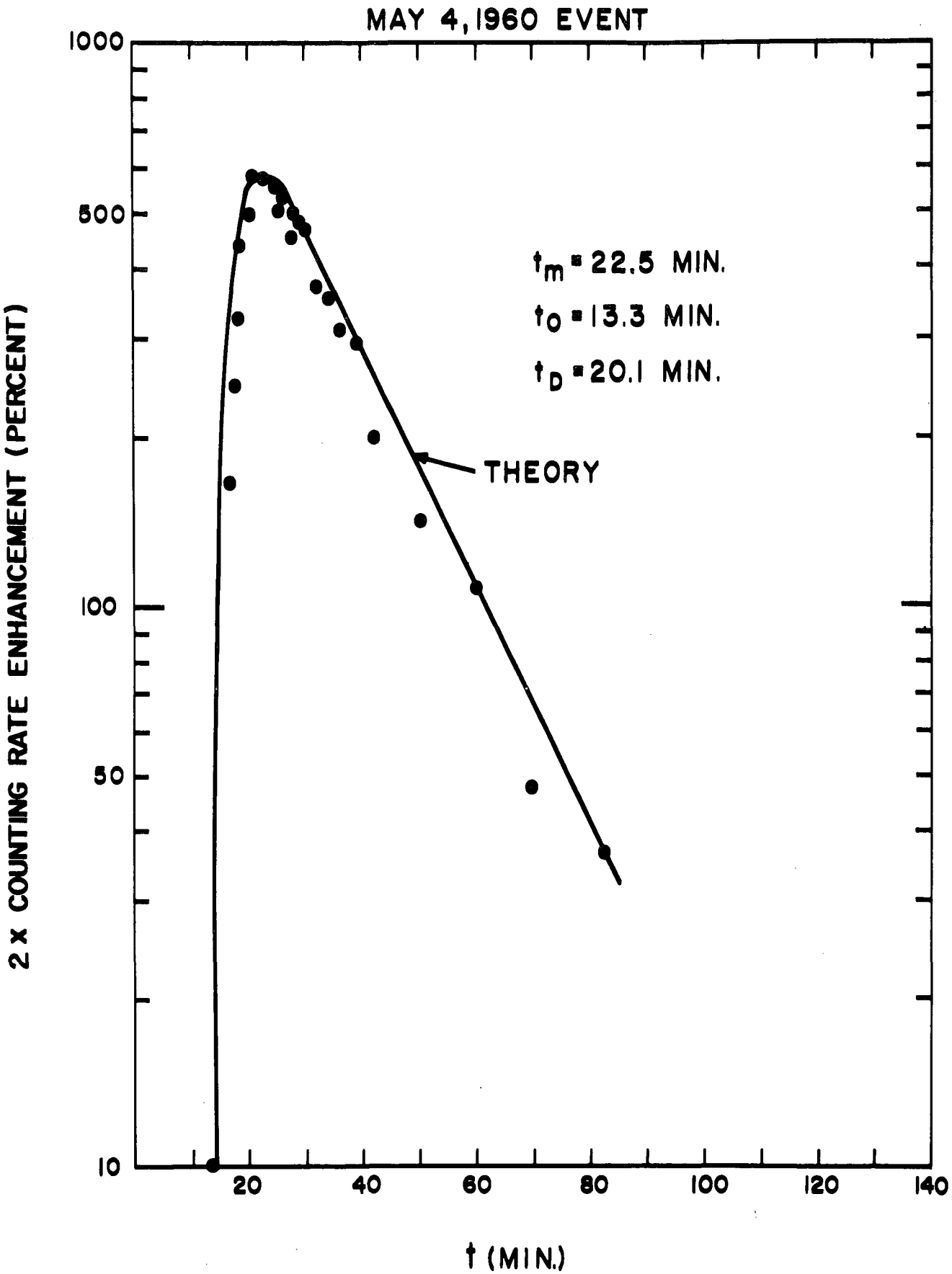
MAY 4, 1960 EVENT
1000
500
100
50
10
20
40
60
80
100
120
140
2 x COUNTING RATE ENHANCEMENT (PERCENT)
t (MIN.)
t_m = 22.5 MIN.
t_0 = 13.3 MIN.
t_D = 20.1 MIN.
THEORY

Figure 11

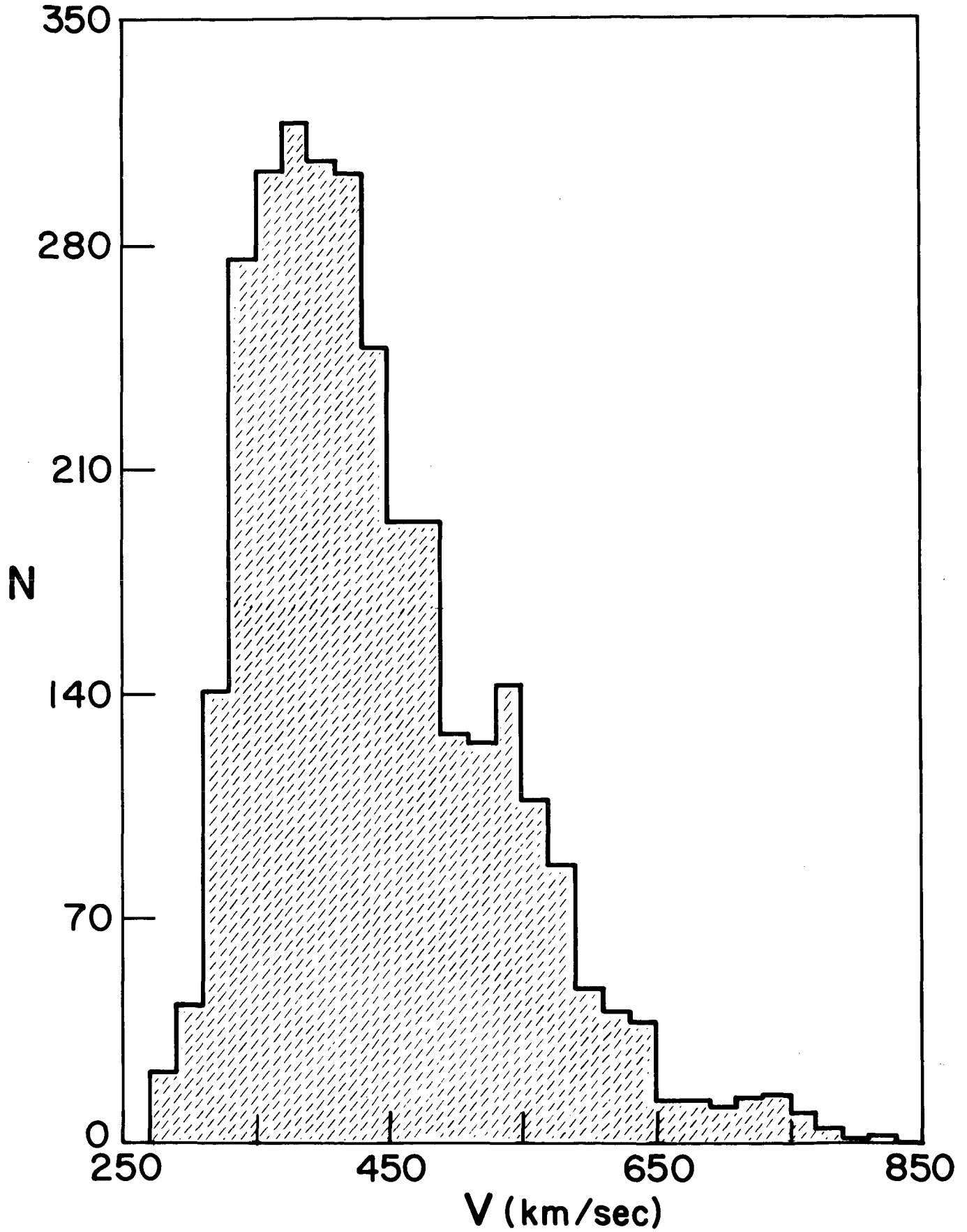

Figure 12

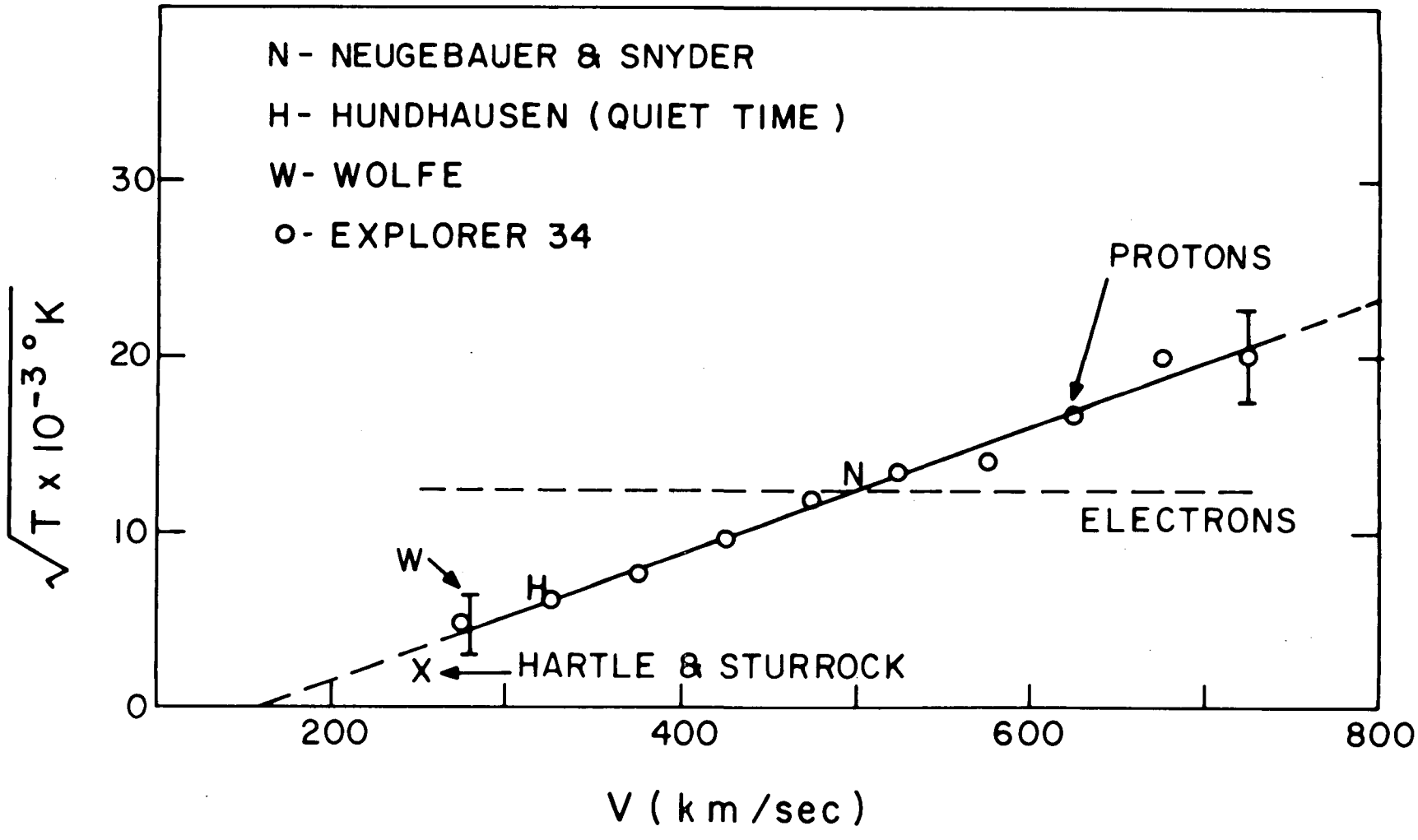
N - NEUGEBAUER & SNYDER
H - HUNDHAUSEN (QUIET TIME)
W - WOLFE
o - EXPLORER 34
PROTONS
ELECTRONS
N
H
W
X
HARTLE & STURROCK
√T x 10⁻³ °K
V (km/sec)
0
10
20
30
200
400
600
800

Figure 13

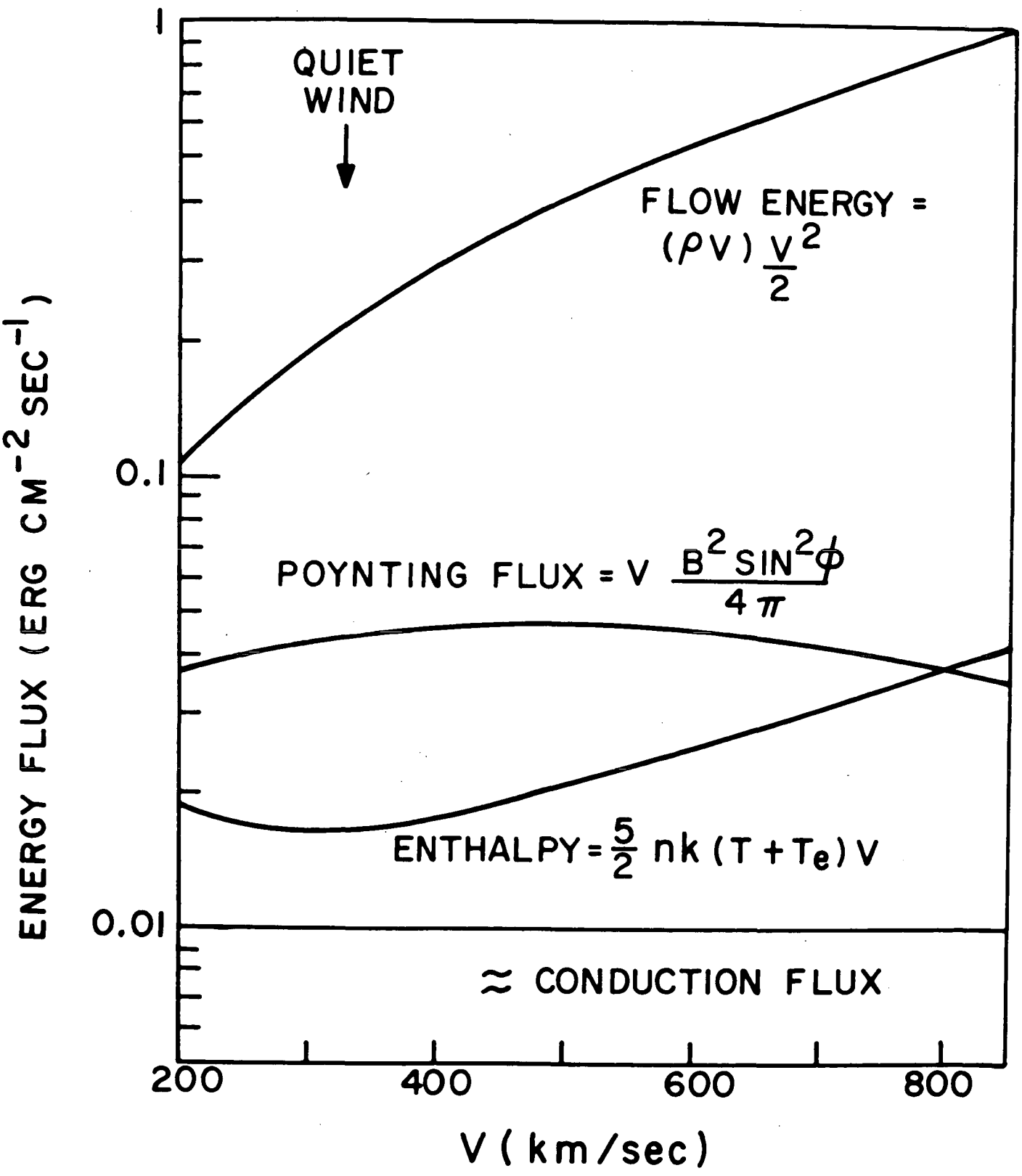
1
0.1
0.01
QUIET
WIND
FLOW ENERGY =
$(\rho V)\frac{V^2}{2}$
POYNTING FLUX = $V\frac{B^2 \sin^2\phi}{4\pi}$
ENTHALPY = $\frac{5}{2} nk(T+T_e)V$
≈ CONDUCTION FLUX
200
400
600
800
V (km/sec)
ENERGY FLUX (ERG CM^{-2} SEC^{-1})

Figure 14

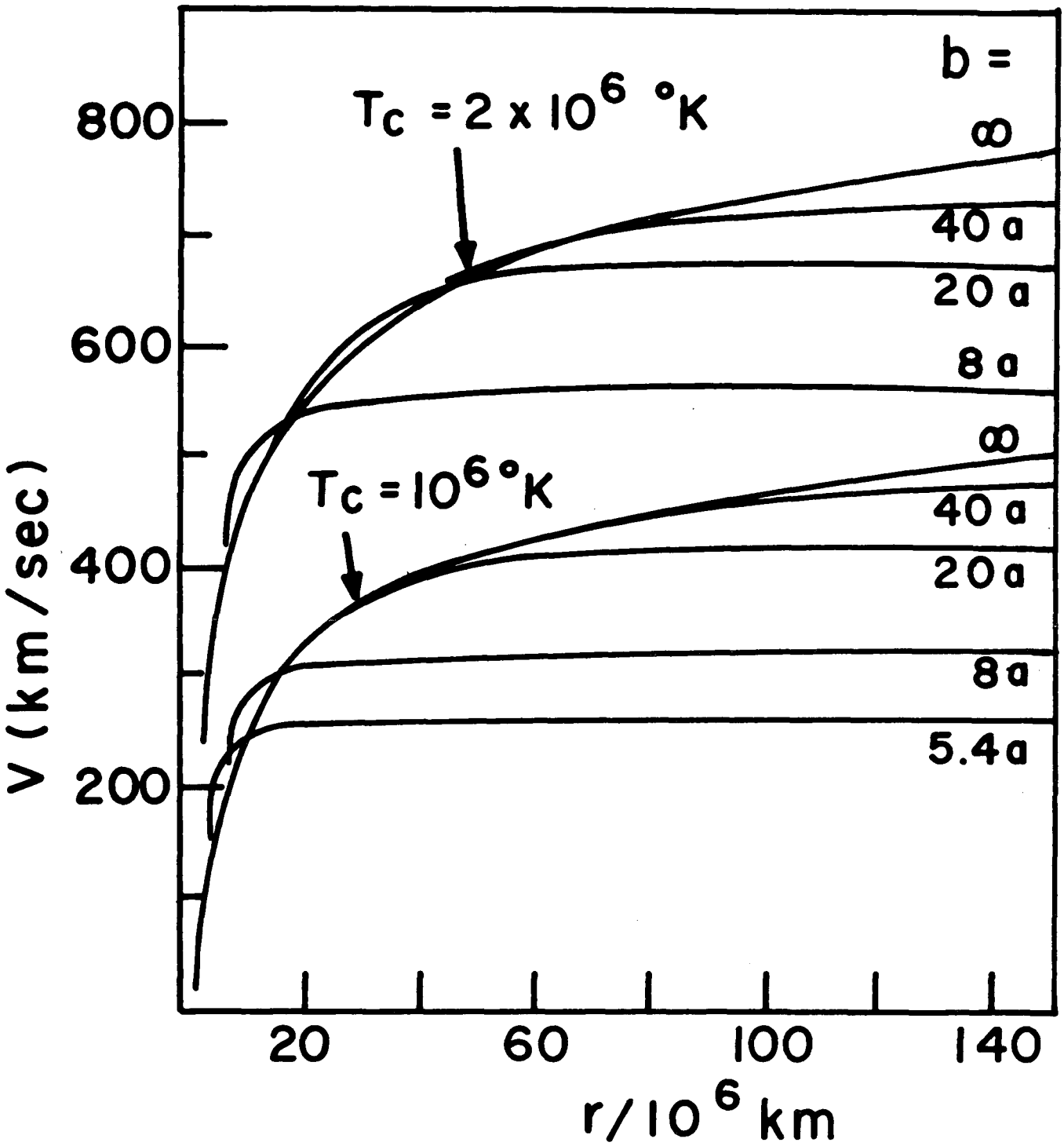
b =
$T_c = 2 \times 10^6$ °K
∞
40 a
20 a
8 a
$T_c = 10^6$ °K
∞
40 a
20 a
8 a
5.4 a
800
600
400
200
V (km/sec)
20
60
100
140
$r/10^6$ km

Figure 15

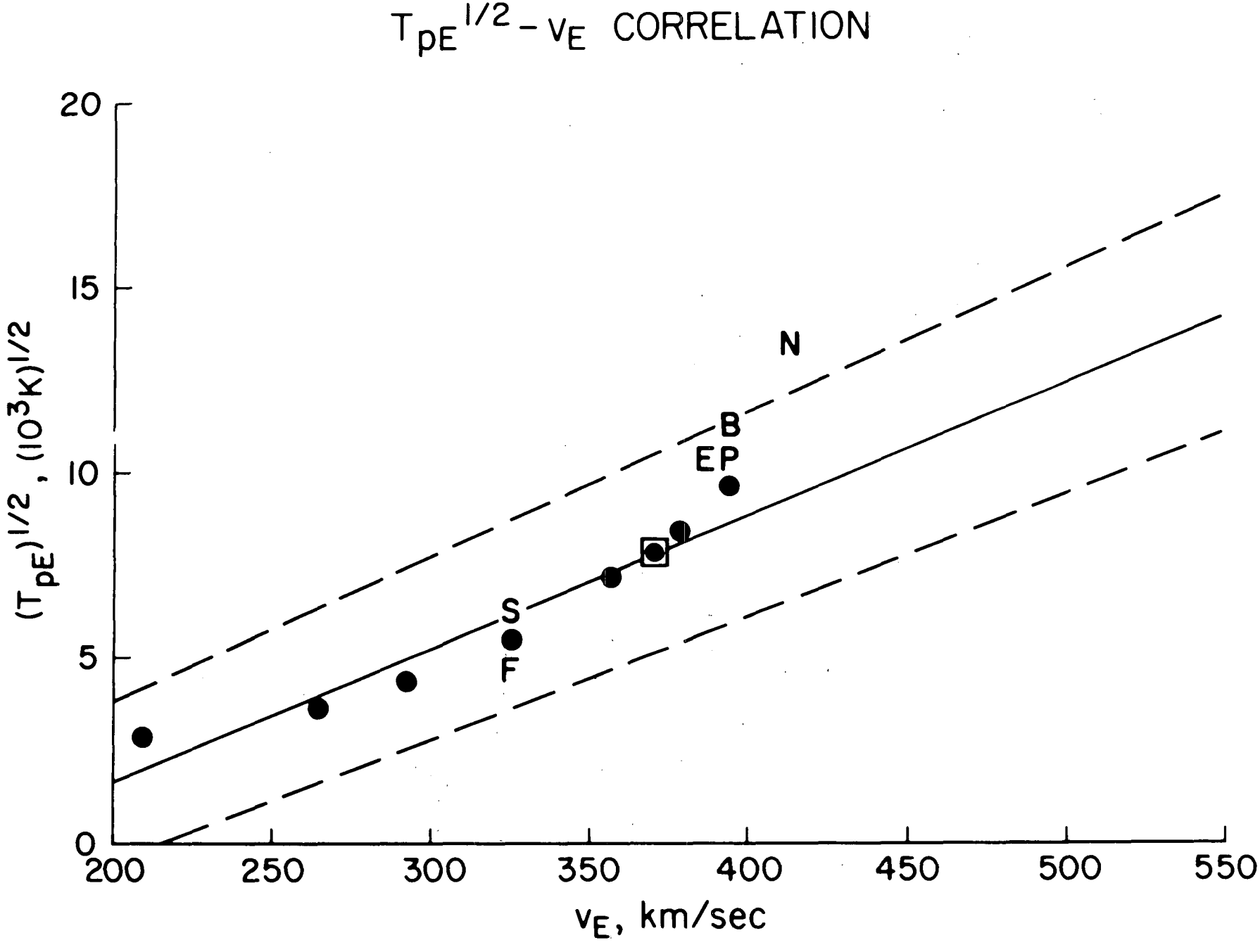
$T_{pE}^{1/2} - v_E$ CORRELATION
$(T_{pE})^{1/2}, (10^3 K)^{1/2}$
v_E, km/sec
0
5
10
15
20
200
250
300
350
400
450
500
550
N
B
EP
S
F

Figure 16

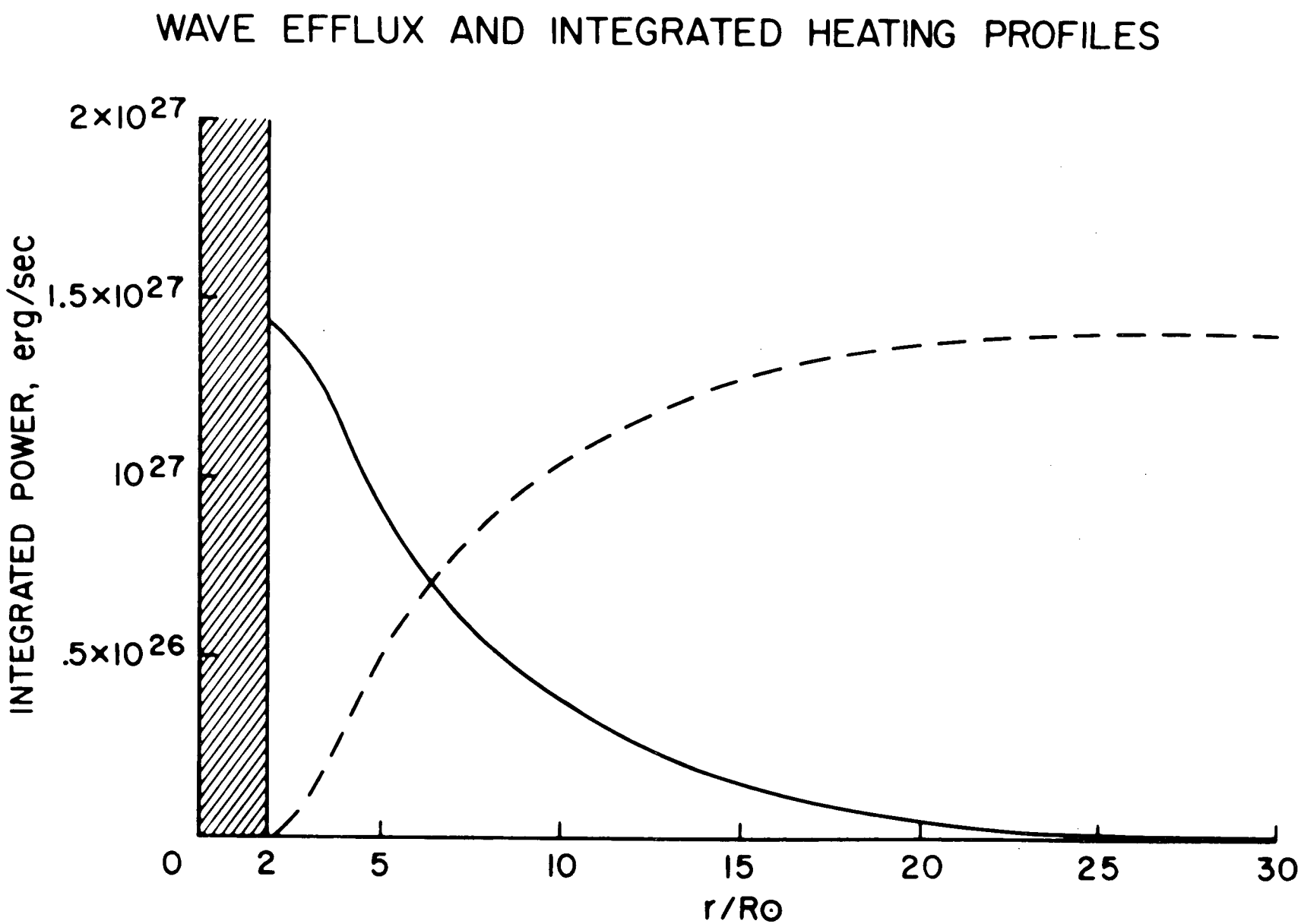
WAVE EFFLUX AND INTEGRATED HEATING PROFILES
INTEGRATED POWER, erg/sec
2×10^27
1.5×10^27
10^27
.5×10^26
0
2
5
10
15
20
25
30
r/Ro

Figure 17

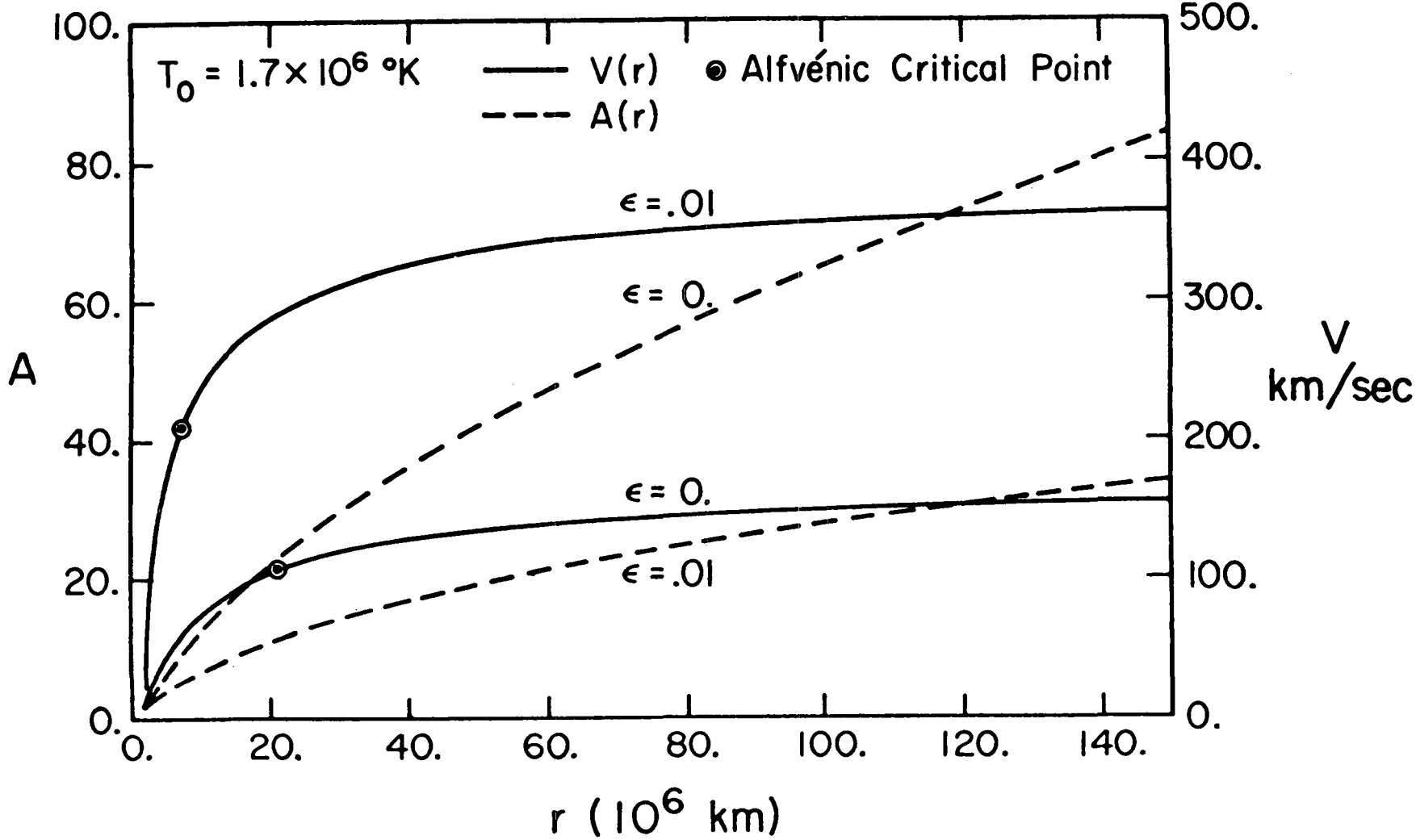

The amplification coefficient A and the solar wind velocity V as functions of r for a fixed value of T_o and two values of ε (0. and .01).

Figure 18

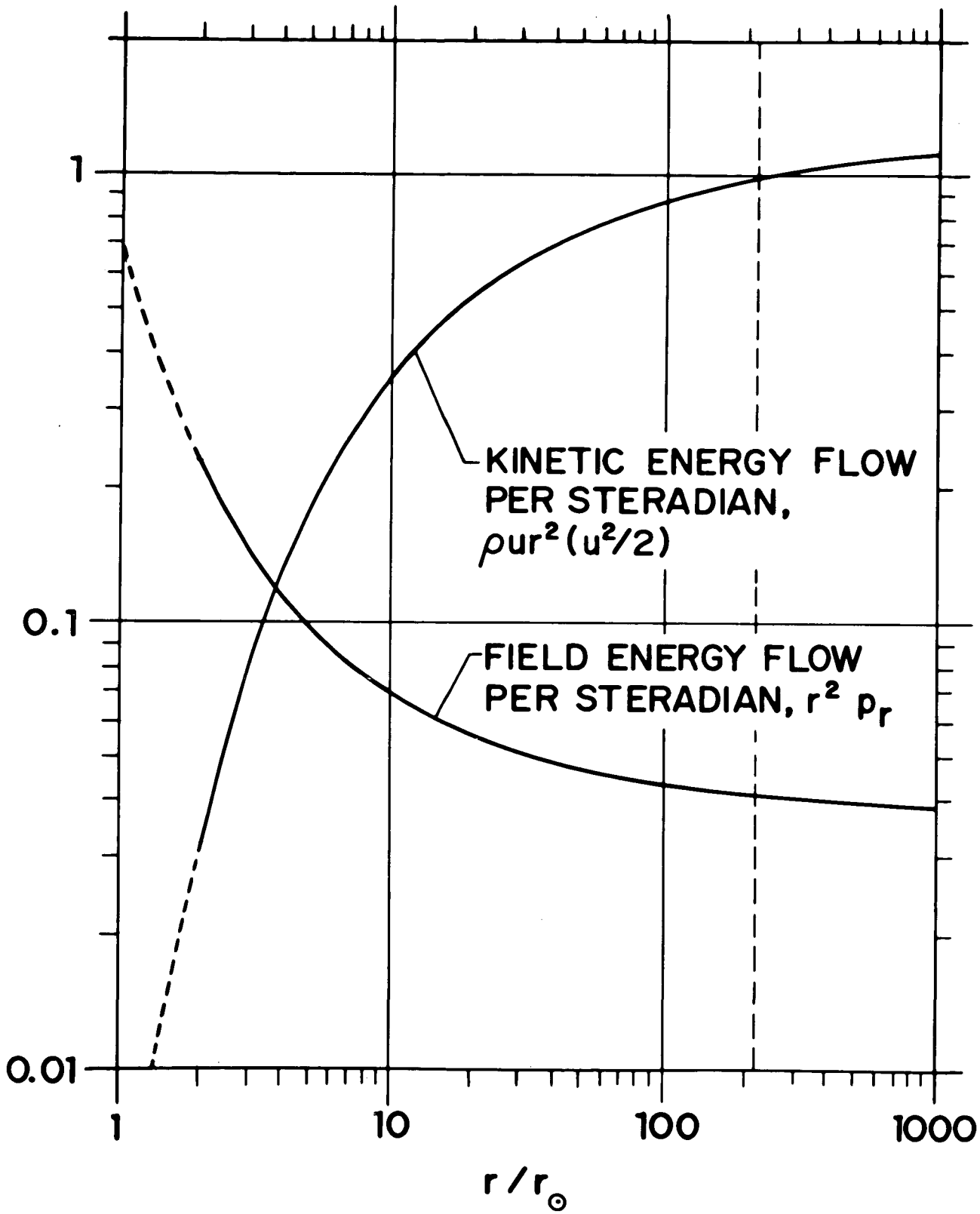
1
0.1
0.01
KINETIC ENERGY FLOW
PER STERADIAN,
ρur² (u²/2)
FIELD ENERGY FLOW
PER STERADIAN, r² p_r
1
10
100
1000
r / r_⊙

Figure 19

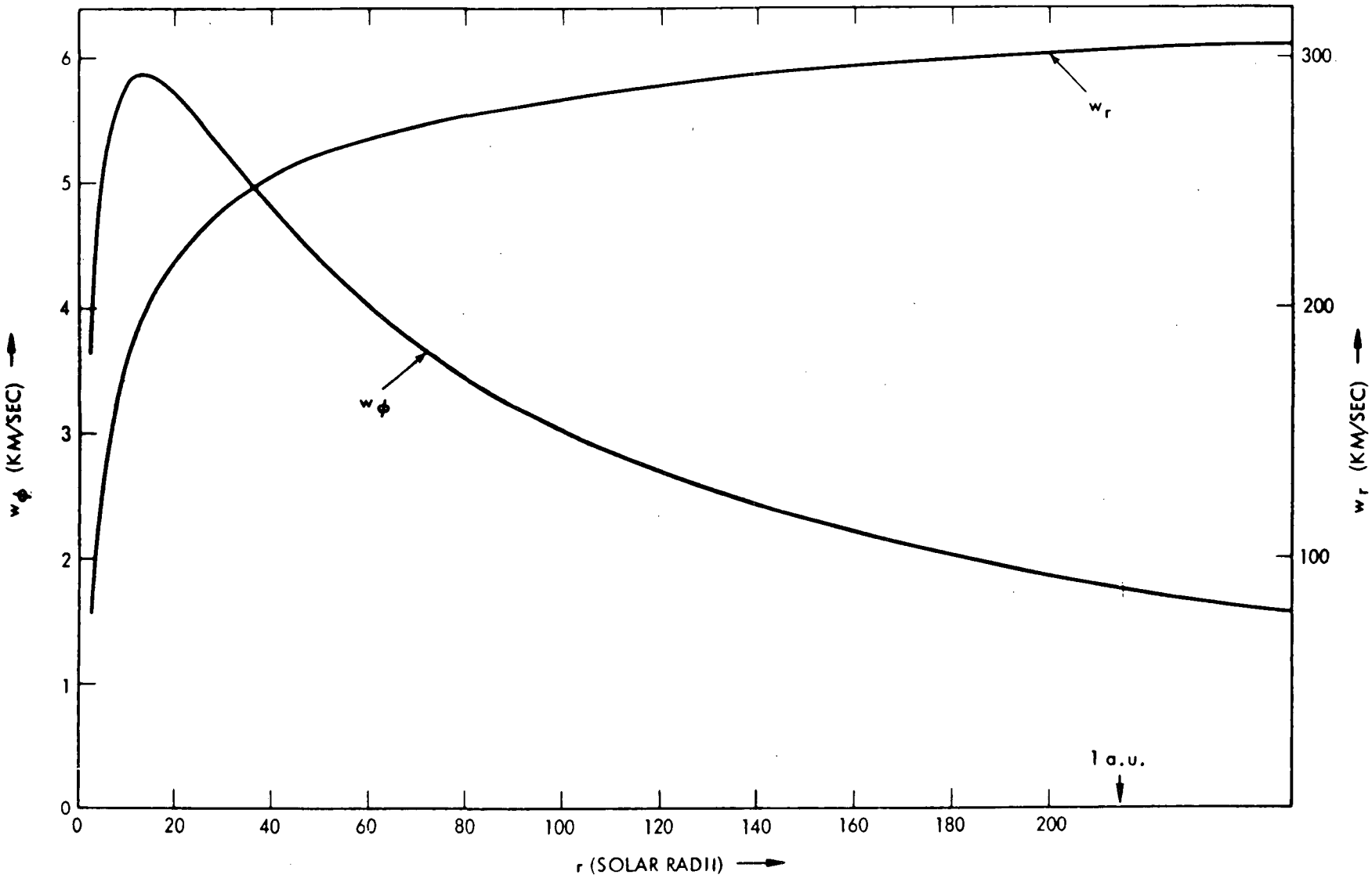
6
5
4
3
2
1
0
300
200
100
w_ϕ (KM/SEC)
w_r (KM/SEC)
w_r
w_ϕ
1 a.u.
0
20
40
60
80
100
120
140
160
180
200
r (SOLAR RADII)

Figure 20